

Reference

NBS  
Publi-  
cations

NAT'L INST. OF STAND & TECH



A11105 974149



NBS TECHNICAL NOTE **1150**

U.S. DEPARTMENT OF COMMERCE/National Bureau of Standards

# Mathematical Models for the Corrosion Protective Performance of Organic Coatings

QC

100

.U5753

1150

1982

## NATIONAL BUREAU OF STANDARDS

The National Bureau of Standards<sup>1</sup> was established by an act of Congress on March 3, 1901. The Bureau's overall goal is to strengthen and advance the Nation's science and technology and facilitate their effective application for public benefit. To this end, the Bureau conducts research and provides: (1) a basis for the Nation's physical measurement system, (2) scientific and technological services for industry and government, (3) a technical basis for equity in trade, and (4) technical services to promote public safety. The Bureau's technical work is performed by the National Measurement Laboratory, the National Engineering Laboratory, and the Institute for Computer Sciences and Technology.

**THE NATIONAL MEASUREMENT LABORATORY** provides the national system of physical and chemical and materials measurement; coordinates the system with measurement systems of other nations and furnishes essential services leading to accurate and uniform physical and chemical measurement throughout the Nation's scientific community, industry, and commerce; conducts materials research leading to improved methods of measurement, standards, and data on the properties of materials needed by industry, commerce, educational institutions, and Government; provides advisory and research services to other Government agencies; develops, produces, and distributes Standard Reference Materials; and provides calibration services. The Laboratory consists of the following centers:

Absolute Physical Quantities<sup>2</sup> — Radiation Research — Chemical Physics —  
Analytical Chemistry — Materials Science

**THE NATIONAL ENGINEERING LABORATORY** provides technology and technical services to the public and private sectors to address national needs and to solve national problems; conducts research in engineering and applied science in support of these efforts; builds and maintains competence in the necessary disciplines required to carry out this research and technical service; develops engineering data and measurement capabilities; provides engineering measurement traceability services; develops test methods and proposes engineering standards and code changes; develops and proposes new engineering practices; and develops and improves mechanisms to transfer results of its research to the ultimate user. The Laboratory consists of the following centers:

Applied Mathematics — Electronics and Electrical Engineering<sup>2</sup> — Manufacturing Engineering — Building Technology — Fire Research — Chemical Engineering<sup>2</sup>

**THE INSTITUTE FOR COMPUTER SCIENCES AND TECHNOLOGY** conducts research and provides scientific and technical services to aid Federal agencies in the selection, acquisition, application, and use of computer technology to improve effectiveness and economy in Government operations in accordance with Public Law 89-306 (40 U.S.C. 759), relevant Executive Orders, and other directives; carries out this mission by managing the Federal Information Processing Standards Program, developing Federal ADP standards guidelines, and managing Federal participation in ADP voluntary standardization activities; provides scientific and technological advisory services and assistance to Federal agencies; and provides the technical foundation for computer-related policies of the Federal Government. The Institute consists of the following centers:

Programming Science and Technology — Computer Systems Engineering.

<sup>1</sup>Headquarters and Laboratories at Gaithersburg, MD, unless otherwise noted; mailing address Washington, DC 20234.

<sup>2</sup>Some divisions within the center are located at Boulder, CO 80303.

# Mathematical Models for the Corrosion Protective Performance of Organic Coatings

---

James M. Pommersheim  
Department of Chemical Engineering  
Bucknell University  
Lewisburg, PA 17837

National Bureau of Standards

SEP 30 1982

and

Paul G. Campbell and Mary E. McKnight  
Center for Building Technology  
National Engineering Laboratory  
National Bureau of Standards  
Washington, DC 20234

100-1150  
20700  
115713  
100-1150  
1982



---

U.S. DEPARTMENT OF COMMERCE, Malcolm Baldrige, Secretary  
NATIONAL BUREAU OF STANDARDS, Ernest Ambler, Director  
Issued September 1982

INTRODUCTION TO THE SERIES

SEPTEMBER 1982

National Bureau of Standards Technical Note 1150  
Natl. Bur. Stand. (U.S.), Tech. Note 1150, 99 pages (Sept. 1982)  
CODEN:NBTNAE

U.S. GOVERNMENT PRINTING OFFICE  
WASHINGTON: 1982

---

For sale by the Superintendent of Documents, U.S. Government Printing Office, Washington, D.C. 20402  
Price \$5.50  
(Add 25 percent for other than U.S. mailing)

TABLE OF CONTENTS

	<u>Page</u>
LIST OF TABLES. . . . .	v
LIST OF FIGURES . . . . .	vi
ABSTRACT. . . . .	vii
1. INTRODUCTION . . . . .	1
2. CONCEPTUAL MODELS. . . . .	3
2.1 Water and Oxygen Permeability . . . . .	3
2.2 Blister Formation and Growth. . . . .	4
2.3 Corrosion Phenomena . . . . .	5
3. MATHEMATICAL MODELS. . . . .	9
3.1 Water and Oxygen Permeability . . . . .	9
3.1.1 Volume Balance . . . . .	10
3.1.2 Rate Laws for Sorption and Diffusion . . . . .	11
3.1.2.1 Rate Laws for Sorption (Solubilities) . . . . .	11
3.1.2.2 Rate Laws for Diffusion . . . . .	12
3.1.3 Conservation Balances. . . . .	14
3.1.4 Model Solutions. . . . .	16
3.2 Blister Formation and Growth. . . . .	22
3.2.1 Blister Growth - Concentrated Spots of Impurity. . . . .	28
3.2.2 Blister Growth - Uniform Distribution of Impurity. . . . .	31
3.3 Corrosion Phenomena . . . . .	33
3.3.1 Potential Difference Model . . . . .	35
3.3.2 Equivalent Circuit Model . . . . .	37
4. DISCUSSION OF RESULTS. . . . .	46
4.1 Water and Oxygen Permeability . . . . .	46
4.2 Blister Formation and Growth. . . . .	51
4.3 Corrosion Phenomena . . . . .	56
5. SUMMARY AND CONCLUSIONS. . . . .	60

	<u>Page</u>
6. NOMENCLATURE . . . . .	65
7. REFERENCES . . . . .	69

APPENDICES

A. SOLUTION TO THE MATHEMATICAL MODEL FOR DIFFUSION OF OXYGEN AND WATER THROUGH ORGANIC COATINGS . . . . .	70
A.1 Long Time Model Solutions . . . . .	72
A.2 Short Time Model Solutions. . . . .	77
B. SOLUTION TO THE MATHEMATICAL MODEL FOR CORROSION PHENOMENA BENEATH AN ORGANIC COATING . . . . .	81
B.1 Potential Difference Model. . . . .	81
B.2 Equivalent Circuit Models . . . . .	84
B.2.1 Constant Product Resistance. . . . .	85
B.2.2 Langmuir Adsorption of Corrosion Products. . . . .	86
B.2.3 Accumulation of Solid Products . . . . .	89

LIST OF TABLES

<u>Table No.</u>		<u>Page</u>
1	Concentration of Water and Oxygen in Organic Coatings (Summary of Models) . . . . .	19
2	Assumptions of the Mathematical Models for Blister Growth . . .	26

LIST OF FIGURES

<u>Figure No.</u>		<u>Page</u>
1	Schematic Representation (Cross-Section) of Organic Polymer Coating. . . . .	2
2	Schematic Representation of a Blister Within an Organic Coating. . . . .	24
2A	Concentrated Spot of Impurity. . . . .	24
2B	Uniform Distribution of Impurity . . . . .	24
3	Equivalent Electrical Circuit for Polarization. . . . .	38

## ABSTRACT

Mathematical models were developed for conceptual models describing the principal phenomena that occur in the corrosion performance of polymeric coatings. These include models for water and oxygen permeability through organic coatings, models for the growth of blisters beneath coatings, and preliminary models for the polarization occurring at the electrode surfaces. Results predicted by the models are discussed in terms of the improvement of the protective function of the membrane.

Keywords: absorption; adhesion; adsorption; conceptual models; corrosion; mathematical models; organic coating; osmosis; osmotic pressure; oxygen; permeability; pigment; protective performance; substrate; vehicle; water.



## 1. INTRODUCTION

In order to assess the corrosion protective performance of organic coatings the phenomena that lead to corrosion must be understood. Corrosion itself is the destruction of a metal surface by electrochemical action. Aqueous corrosion occurs when three things are present: oxygen, water and an electrolyte. There will be no corrosion unless all three are present at the corrosion site.

Figure 1 shows a cross-section of a typical organic coating. A coating having a uniform thickness  $L$  (typically 0.1 mm) covers a metal substrate. The organic coating consists of a vehicle (or binder) phase and a particle (or pigment) phase. Water and oxygen can penetrate through the coating to the surface of the substrate. The rate of passage of the penetrants (water and oxygen) will depend on many factors: the availability at the coating surface, their solubility in the coating, their diffusivity through the coating, their affinity for the pigment particles their rate of consumption at the corrosion site and the osmotic pressure of the electrolyte-membrane combination. In addition to depending on the chemical and physical nature of the organic coating used, all of these factors are temperature sensitive.

The electrolyte can be a foreign ion such as chloride or sulfate or it can be the corrosion products themselves. Since corrosion does not begin without an electrolyte, a foreign ion must be initially present as an impurity on the metal surface, or as a leachable ion present in the coating, or as an ion present in an external aqueous environment which can diffuse through the coating to the metal surface. In most applications, the surface of the metal is not perfectly clean and an accumulation of impurity ions may initiate

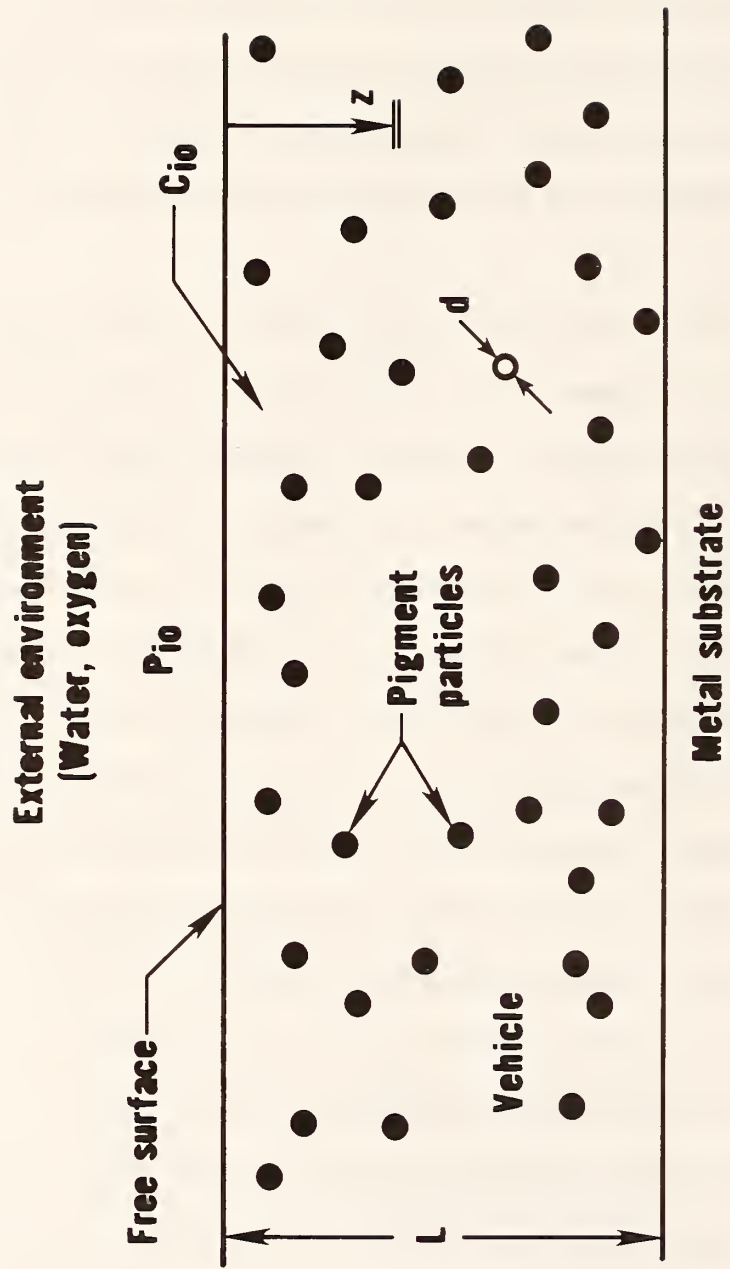


Figure 1: Schematic Representation (Cross-Section) of Organic Polymer Coating

localized corrosion there. The presence of these ions leads to osmotic pressure differences between the inside and outside of the coating. This augments the diffusion of water through the coating and can lead to the formation of blisters at the metal surface.

In this paper, the key conceptual phenomena affecting the corrosion protective performance of organic coatings are discussed, and mathematical models describing these phenomena are formulated and solved.

## 2. CONCEPTUAL MODELS

The model for corrosion protective performance of organic coatings was conceived in terms of three different conceptual sub-models:

- (i) submodel for water and oxygen permeability
- (ii) submodel for blister formation and growth
- (iii) submodel for corrosion phenomena

### 2.1 Water and Oxygen Permeability

Both water and an oxidizing chemical species must be present at the metal surface in order for corrosion to occur. Compounds like halogens, sulfur dioxide and oxygen can all serve as oxidizers but molecular oxygen is by far the most prevalent. The organic coating (refer to Figure 1) serves as a barrier to the diffusion of water and oxygen. If the coating were not present they would have ready access to the metal surface. The presence of the coating helps prevent the initiation of corrosion, and, in addition, slows down the rate of corrosion once it has begun. Most coatings, are relatively permeable to the penetration of water and oxygen, especially water [1]. To arrive at the metal surface both water and oxygen must first dissolve (or absorb) into the outside of the coating and then diffuse through the coating towards the

metallic corrosion site. Some of the water and oxygen does not arrive at the metal surface since they are absorbed within the coating. In addition some will not arrive because it will be adsorbed by the pigment particles within the coating.

For a given type of organic coating, metal substrate and corrosive environment, the overall permeation of the organic coating to oxygen and water depends on the concentrations of oxygen and water outside the coating, the thickness of the coating, the solubility of the compounds into the film, the diffusivity through the film, the pigment to vehicle ratio, the pigment size and shape, and the temperature. With more pigment particles, it is more difficult for species to diffuse. At the same time, more retention of penetrants occurs because of the greater particle density. Thus, raising the pigment to vehicle ratio will lower the permeation by lowering the diffusivity and increasing the amount of adsorption within the coating. Imperfect wetting or adhesion of the binder to the pigment particles during formulation of the coating can also give rise to pockets surrounding the particles into which adsorbed water and oxygen can go. Raising the temperature will raise the diffusivity, lower the solubility, and raise the adsorption. For most coatings the overall permeability of the film increases with increasing temperature [2]. This indicates that the diffusion coefficient or diffusivity of the oxygen and water through the film are temperature sensitive parameters.

## 2.2 Blister Formation and Growth

When water has first penetrated through to the metal surface it mixes with impurity ions present at the surface and small liquid cells of locally high concentration are formed. The large anions there, typically  $\text{Cl}^-$  and

$\text{SO}_4^{=}$ , cannot diffuse out through the coating, which now acts as a semipermeable membrane. Alkali pigments can supply additional species to the anion pool within the blister and may change the nature of the corrosion process. Osmotic pressure builds up and more water diffuses into the cells, gradually enlarging them. In regions where the adhesion between the coating and the metal is poor, or where the concentration of impurity is especially high, the coating can disbond from the metal substrate and a blister can form. The blister continues to enlarge but at a slower and slower rate as the impurity ion is diluted and the osmotic pressure drops. If the enlarging blister exposes additional amounts of surface impurity ions, the rate of blister growth does not decrease as fast. A similar effect will occur when ionic corrosion products (such as hydroxyl ions) are formed adjacent to the blister.

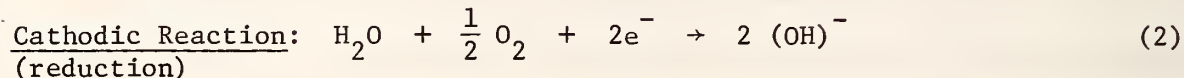
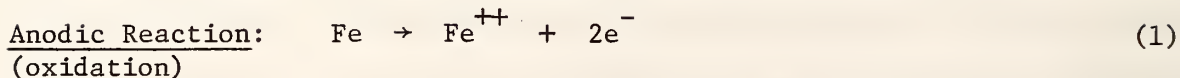
In general, blister growth is slow enough that it is not limited by the availability of water. The blister formation and initial water incursion problems are uncoupled since they do not occur on the same time scale. Of course, water permeability (refer to previous section) is essential to the initiation of the cells which lead to the formation of blisters.

After sufficient time, the blisters may enlarge to such a point that adjacent blisters link together. This can lead to complete detachment of the coating from the substrate causing failure of the organic coating.

### 2.3 Corrosion Phenomena

Corrosion reactions initiate when oxygen, water and ions are present locally at the metal surface either in a detached film or within a blister.

For iron-based metals, the most common half-cell reactions are:



The anodic and cathodic reactions occur at different sites on the metal surface. The electrons released in the anodic reactions travel through the metal to the location of the cathode. This completes the circuit. Electron flow is retarded (or equivalently, circuit resistance is increased) by several mechanisms. These include:

- 1) Build-up of oxide layers or layers of other solid corrosion products such as  $\text{Fe}(\text{OH})_3$  or  $\text{Fe}_2\text{O}_3$ .
- 2) Formation of an electrical double layer adjacent to the metal surface.
- 3) Formation of gases such as hydrogen at the cathode surface or oxygen at the anode surface.
- 4) Adsorption of hydrogen or oxygen ions which result in an overvoltage because of polarization of the anode or cathode.

The anodic and cathodic sites may shift over the surface with time as the coating becomes detached. This can permit substantially uniform corrosion to occur. The liquid films of corrosion products formed beneath detached coatings may be basic [3].

With a blistered surface, the anodic reaction is more likely to occur in the center of a blister where a pit may subsequently develop. The cathodic reaction is more likely to occur at the periphery of the blister where the oxygen needed for this reaction is more readily accessible to depolarize the cathode. The locally high basicity generated by the formation of hydroxyl ions can weaken the coating near the cathode surface. Accumulation of solid

corrosion products at the cathode surface also occurs. Both factors can cause "cathodic delamination" with more rapid coating detachment than would otherwise be observed.

For the half-cell reactions considered, the principal solid corrosion product is ferric hydroxide,  $\text{Fe}(\text{OH})_3$ . The original corrosion product is ferrous hydroxide,  $\text{Fe}(\text{OH})_2$ , which forms when ferrous,  $\text{Fe}^{++}$ , and hydroxyl,  $(\text{OH})^-$ , ions diffuse towards one another through solution. Ferrous hydroxide undergoes further oxidation to ferric hydroxide. In strongly oxidative environments, films of ferric oxide ( $\text{Fe}_2\text{O}_3$ ) also form. The corrosion products can build-up uniformly as may occur under a detached film, or they may precipitate closer to the cathode than to the anode as can occur with a blistered coating.

Corrosion is viewed as being basically an electrochemical phenomenon. The rate of corrosion is considered to be a function of the electromotive force and the resistance of the circuit. The greater the potential between the anode and cathode the greater is the driving force for corrosion. The driving force is initially proportional to the potential as determined by the galvanic series for the metal in solution. As corrosion proceeds, the potential difference between the anode and cathode decreases and the accumulating corrosion products cut down on the electron flow. The potential of the cathode slowly drifts towards that of the anode (cathodic polarization), while the potential of the anode drifts slowly towards that of the cathode (anodic polarization). In general, cathodic polarization exerts more of a controlling influence on the overall corrosion process than does anodic polarization. For example, when hydrogen adsorbs at the cathode it can polarize the surface reducing the electron flow and thus decreasing corrosion at the anode.

Corrosion can be accelerated again if oxygen is introduced into the system. In this case, adsorbed hydrogen ions are removed from the cathode surface by the reaction:



Corrosion increases because the cathode potential drops, increasing the driving force between the cathode and anode and raising the electron flow. Oxygen in this case acts as a cathodic depolarizer.

The area of the cathode surface relative to that of the anode is also an important parameter in corrosion models. Returning to the previous example, the hydrogen ions reaching a large cathode will be spread out over a larger area than with a small cathode and are easier to remove by reaction (3). Thus, in oxidative environments, such as those present beneath a corrosion protective coating, an enlarging cathode contributes to accelerated corrosion rates.

The corrosion phenomena can also be viewed as being part of an electrical circuit. The difference in potential between the anode and cathode create an electron flow which passes through several series resistances. These include the resistance of the electrolyte, the resistance of the corrosion products and the resistance of the metal itself. For isothermal systems, the metal resistance remains constant and should be low. Corrosion product resistance increases with time as the products accumulate (either as an electrical double layer, adsorbed gases, or solid products).

The electrical double layer that forms at the cathode consists of an inner layer of oriented water dipoles next to the electrode surface and an

outer layer of solvated ions in solution (outer Helmholtz plane). These layers provide additional resistance by slowing down the electron flow. This cathodic polarization decreases the circuit potential. Eventually the resistance provided by the double layer approaches some limit or ultimate value and the potential differences between the anode and the cathode also become constant. Solid films of corrosion products can cause similar effects.

The resistance provided by the conducting solution can also slowly change as its composition changes. As ion concentrations increase, the higher ionic mobilities which result lower the electrolyte resistance. However, it can still be an appreciable part of the total circuit resistance, especially in solutions which remain relatively dilute.

### 3. MATHEMATICAL MODELS

The overall mathematical model for the corrosion protective performance of organic coatings was formulated based upon the previously developed conceptual model describing the principal phenomena that occur. Mathematical sub-models were developed for each of the conceptual models discussed in the previous section. These included mathematical sub-models for water and oxygen permeability, for blister formation and growth, and for the corrosion phenomenon itself.

#### 3.1 Water and Oxygen Permeability

Since water and oxygen must be present at the metal surface in order for corrosion to occur, it is important to know the rate at which they pass through the coating. Mathematical models for this process are based on a

knowledge of the rate laws for absorption and adsorption and diffusion and the mass conservation balances for water and oxygen. Input to the conservation balances consists of the rate laws for absorption into the surface of the coating, for diffusion through the coating and for adsorption on the surface of the pigment particles. The rate laws and conservation equations must both account for the effect of the pigment particles on the permeation process.

### 3.1.1 Volume Balance

The relations between pigment to vehicle ratio, pigment particle size, and volume fraction vehicle (porosity) can be determined by making an overall volume balance on the coating.

Consider the system depicted in figure 1. Pigment particles of uniform size are evenly dispersed throughout the coating. The coating thickness is  $L$ .  $Z$  is the coating depth measured normal to the free surface.  $n$ , the number density of particles, or pigment particles per unit volume of coating, is calculable from the relation:

$$n = \frac{6}{\pi} \frac{1 - \epsilon}{d^3} \quad (1)$$

where  $(1 - \epsilon)$  is the volume fraction of the pigment particles and  $d$  is their diameter (equivalent sphere). If the porosity  $\epsilon$  (volume fraction vehicle) is unknown it can be found by making a volume balance on the coating:

$$\epsilon = \frac{1}{1 + (p/v) (\rho_v / \rho_p)} \quad (2)$$

where  $(p/v)$  is the pigment to vehicle weight ratio and  $\rho_v / \rho_p$  is the density ratio.

### 3.1.2 Rate Laws for Sorption and Diffusion

#### 3.1.2.1 Rate Laws for Sorption (Solubilities)

Absorption into the coating surface was assumed to follow Henry's law which states that the solubility into the coating is proportional to the concentration (or partial pressure) of penetrant in the external phase outside the coating. This presumes that there is an equilibrium between phases at the interface. For coatings exposed to vapors, the constant of proportionality is the Henry's law constant  $H_i$ . Thus:

$$p_{i0} = H_i C_{i0} \quad (3)$$

where

$p_{i0}$  is the partial pressure of component  $i$  in the external phase

$C_{i0}$  is the concentration of penetrant  $i$  just inside the coating surface ( $Z = 0$ ).

For coatings exposed to liquids, a similar equation applies. Aqueous systems favor the penetration of water through the coating while vapor systems favor the penetration of oxygen. At higher humidities in vapor systems, the penetration of water increases because of the higher partial pressure of water. Oxygen transfer to organic coatings in aqueous systems increases as the amount of oxygen dissolved in the liquid increases. In any case, as a result of exposure to the external environment, it is presumed that a constant concentration of penetrant  $C_{i0}$  is present just inside the coating. It is

important to re-emphasize that if either oxygen or water are absent from the external phase, only a negligible amount of corrosion occurs since  $C_{i0} = 0$ .

Within the coating, pigment particles also have an affinity for water and oxygen. For a single pigment particle, the water and oxygen present in the vicinity of its surface adsorb on the surface at a rate proportional to the product of the particle's surface area ( $S_p$ ) and the concentration of penetrant ( $C_i$ ) present in the vehicle near the pigment particle. Thus:

$$-r_{is} = k_{ai} S_p C_i \quad (4)$$

where

$r_{is}$  is the rate of adsorption of penetrant  $i$  per particle

and

$k_{ai}$  is the adsorption rate constant for penetrant  $i$ .

### 3.1.2.2 Rate Laws for Diffusion

The diffusion of oxygen and water through the coating was based on Fick's Law. This states that the flux of chemical species  $i$ , ( $N_i$ ) is proportional to the concentration gradient. The constant of proportionality in Fick's Law is the diffusion coefficient or diffusivity ( $D_i$ ). Thus:

$$N_i = - D_i \nabla C_i = - D_i \frac{\partial C_i}{\partial Z} \quad (5)$$

In equation (5) the gradient  $\nabla C_i$  is expressed as  $\partial C_i / \partial Z$ . This assumes that diffusion only occurs in the  $Z$  direction. This is a reasonable assumption considering that most coatings are thin and have large flat surfaces which are

exposed to uniform environments. Thus there is little flux across the film in the directions parallel to the surfaces.

The diffusion coefficient  $D_i$  will in general be much less than the molecular or free stream diffusivity of molecules moving unimpeded through solution.  $D_i$  is thus regarded as an effective diffusivity rather than a true diffusion coefficient. The diffusion of molecules is slowed because:

- 1) The effective area of diffusion is lowered due to the presence of the pigment phase.
- 2) The diffusion path between and within the vehicle are tortuous so that it takes longer for a given molecule to pass from one point to another.
- 3) Any given diffusion path has constricted regions (bottlenecks) where there is a greater resistance to the diffusive flow of molecules.

The effects of these constraining factors are mathematically expressed in the relationship [4]:

$$D_i = D_i^* \varepsilon \frac{\sigma}{\tau} \quad (6)$$

where

$D_i^*$  is the molecular (or Knudsen) diffusivity

$\sigma$  is the constriction factor

$\tau$  is the tortuosity factor

The porosity  $\varepsilon$  and constriction factor  $\sigma$  are both less than unity while the tortuosity factor  $\tau$  is greater than unity. All three factors act to lower the actual diffusion coefficient  $D_i$ . In general, equation (6) cannot be used to predict the value of  $D_i$  since the factors on the right hand side of this equation are unknowns which can only be determined from experiments.

Bruggeman [5] has shown theoretically, using an electrical analog model, that  $\sigma/\tau$  varies approximately as  $\sqrt{\epsilon}$ . According to equation (6), this predicts that the diffusion coefficient should vary as  $\epsilon^{3/2}$ . However the useful range of Bruggeman's approximation is only from  $0.4 < \epsilon < 1$ . At lower porosities, the dependence of  $D_i$  on  $\epsilon$  is even more pronounced than  $\epsilon^{3/2}$ , although actual dependence has not been determined theoretically. Greater dependence of the effective diffusivity on the porosity can occur with clumping of pigment particles caused by poor dispersion or nesting of smaller particles within spaces between larger particles.

### 3.1.3 Conservation Balances

The overall conservation equations governing the rate at which water and oxygen penetrate an organic coating and arrive at corrosion sites will depend on the rate laws describing the processes which are occurring within the film. The rate laws comprise a set of constitutive relations which serve as input to the conservation equations.

An overall conservation balance for each penetrant takes the form:

$$\begin{aligned} \text{Rate of Accumulation} &= \text{Rate of Diffusive Input} - \text{Rate of} \\ &\text{Diffusive Output} - \text{Rate of Disappearance by Sorption} \end{aligned} \quad (7)$$

These molar balances are written on the vehicle, so that the pigment is not part of the system. However, the number density of pigment particles is an important parameter since this influences the rate of removal of penetrant by sorption.

Application of equation (7) leads to:

$$\epsilon \frac{\partial C_i}{\partial t} = - \frac{\partial N_i}{\partial Z} - n r_{is} \quad (8)$$

Equation (8) is the conservation equation for species  $i$ . All terms have units of moles of  $i$ /time, volume of vehicle. The term on the left represents the accumulation of penetrant within the vehicle (refer to equation (7)). The first term on the right represents the net influx of penetrant in any local region of the vehicle. The second term on the right gives an expression for the rate at which the penetrant is removed from the vehicle by adsorption.

Substitution into equation (7) of the rate laws for diffusion (equation (5)) and adsorption (equation (4)) and equation (1) for  $n$  results in:

$$\epsilon \frac{\partial C_i}{\partial t} = D_i \frac{\partial^2 C_i}{\partial Z^2} - \frac{6k_{ai}}{d} (1 - \epsilon) C_i \quad (9)$$

In equation (9) it is assumed that the effective diffusivity  $D_i$  is constant. This is a reasonable assumption for most coating systems, since, in general, for any given coating system  $D_i$ , will only be a function of temperature.

Equation (9) is a linear second order non-homogeneous partial differential equation. Its solution gives  $C_i(Z,t)$ , the concentration of penetrant as a function of film depth ( $Z$ ) and time ( $t$ ). In order to effect a solution, it is necessary to specify three conditions; two boundary conditions (on  $Z$ ) and one initial condition (on  $t$ ). These are given by equations (10), (11) and (12), respectively:

$$C_i(0,t) = C_{i0} \quad (10)$$

$$\frac{\partial C_i}{\partial Z}(L,t) = 0 \quad (11)$$

$$C_i(Z,0) = 0 \quad (12)$$

One boundary condition (equation (10)) is written for the outside coating surface (next to the external environment) and one for the coating-metal substrate interface. At the coating surface ( $Z = 0$ ), it is presumed that the concentration  $C_i$  is equal to the solubility  $C_{i0}$  of water (or oxygen) in the vehicle of the organic coating. At the coating-substrate interface ( $Z = L$ ), the flux of water (and oxygen) is equal to zero. This is expressed mathematically by equation (11) and corresponds physically to the fact that the metal surface is an impermeable boundary to diffusion. Equation (12), the initial condition, expresses mathematically the fact that the coating was initially free of water or oxygen.

Equations (9), (10), (11) and (12) comprise the complete mathematical model for permeation. There is one partial differential equation for oxygen and one for water, both having the same form but different parameters. The parameters of the model are  $D_i$ ,  $(p/v)$ ,  $k_{ai}$ ,  $C_{i0}$  and  $d$ .  $D_i$ ,  $k_{ai}$  and  $C_{i0}$  differ for water and oxygen.

#### 3.1.4 Model Solutions

It is important to be able to predict concentration profiles and fluxes within the coating over the entire time range from the point when the pene-

trants first start to reach the metal substrate to the time when corrosion has initiated and a steady-state concentration profile has developed.

Solutions to equation (9) for  $C_i(Z,t)$  can be effected by several different methods. These include:

- a) separation of variables (boundary value methods)
- b) Laplace Transform methods
- c) computer methods

The analytical methods, (a) and (b), are able to show the precise relations between the variables and parameters of the model. In this sense, they are superior to computer methods. Both analytical methods produce solutions expressed as an infinite series of terms, each of which is a function of both time and position. The separation of variables method gives solutions which converge most rapidly at long dimensionless times. This implies that fewer terms in the series are needed for convergence at long times. Laplace Transform methods yield solutions which converge quickest at shorter dimensionless time.

The dimensionless time referred to here can be obtained by expressing equation (9) in terms of dimensionless groups. Such an analysis shows that:

$$t' = \frac{tD_i/L^2}{\epsilon} \quad (13)$$

$t'$  represents the dimensionless time. Equation (13) lumps together the quantities  $t$ ,  $D_i$ ,  $L$  and  $\epsilon$  into a single dimensionless group.  $t'$  is large at long absolute times  $t$ , for small coating thicknesses  $L$ , for large values of the effective diffusion coefficient  $D_i$ , and for films having low porosities.

Penetrant concentrations have been found as a function of depth into the coating and time for both large and small dimensionless times. For both cases concentrations at the coating-metal interface were found. In addition steady state mathematical solutions for penetrant concentrations and solutions in which adsorption is not significant were derived.

The solutions to these different cases are presented below. A summary by equation number is provided in Table 1. Details of the derivations are presented in Appendix A. Further discussion of the solutions obtained is provided in Section 4 of this report. All of the solutions are given in terms of the dimensionless concentration  $C = C_i/C_{i0}$ , expressed as a function of the dimensionless coating depth  $x = Z/L$ , the dimensionless time  $t'$  (equation 13) and the dimensionless adsorption-diffusion constant  $a$ , as defined by (equation 15).

Table 1. Concentration of Water and Oxygen in Organic Coatings (Summary of Models)

<u>Time Region</u>	<u>Within Coating</u>		<u>At Substrate Interface</u>	
	<u>with sorption</u> $C_i(z,t)$	<u>no sorption</u> $C_i(z,t)$	<u>with sorption</u> $C_i(L,t)$	<u>no sorption</u> $C_i(L,t)$
long times	(14) <sup>+</sup>	(16)	(17)	(18)
short times	(19)	(20)	(21)	(22)
steady state ( $t = \infty$ )	(23)	++	(24)	++

+ equation numbers given in parentheses are keyed to the text  
 ++steady state concentration in these cases is  $C_{i0}$

Long Time Model Solutions

Concentration-Time Profiles

$$C = \frac{\cosh a (1-x)}{\cosh a} - \pi \sum_{n=1}^{\infty} \frac{(-1)^{n+1} (2n-1) \exp \left[ -\left[ a^2 + (2n-1)^2 \frac{\pi^2}{4} \right] t' \right] \cos \left[ (2n-1) \frac{\pi}{2} (1-x) \right]}{a^2 + (2n-1)^2 \frac{\pi^2}{4}} \quad (14)$$

where

$$a \equiv L \left[ \frac{6k_{ai}}{dD} \left( \frac{1-\epsilon}{\epsilon} \right) \right]^{1/2} = L \left[ \frac{6k_{ai}}{dD} (p/v) (\rho_v/\rho_p) \right]^{1/2} \quad (15)$$

-Adsorption Insignificant ( $a = 0$ )

$$C = 1 - \frac{4}{\pi} \sum_{n=1}^{\infty} \frac{(-1)^{n+1}}{(2n-1)} \exp \left[ -(2n-1)^2 \frac{\pi^2}{4} t' \right] \cos \left[ (2n-1) \frac{\pi}{2} (1-x) \right] \quad (16)$$

Concentration-History at Metal Substrate Interface ( $x = 1$ )

$$C(1) = \operatorname{sech} a - \pi \sum_{n=1}^{\infty} \frac{(-1)^{n+1} (2n-1) \exp \left[ -\left[ a^2 + (2n-1)^2 \frac{\pi^2}{4} \right] t' \right]}{a^2 + (2n-1)^2 \frac{\pi^2}{4}} \quad (17)$$

-Adsorption Insignificant ( $a = 0$ )

$$C(1) = 1 - \frac{4}{\pi} \sum_{n=1}^{\infty} \frac{(-1)^n}{2n-1} \exp \left[ -\frac{(2n-1)^2 \pi^2}{4} t' \right] \quad (18)$$

## Short Time Model Solutions

### Concentration-Time Profiles

$$\begin{aligned}
 C = & \frac{1}{\sqrt{4\pi}} \sum_{n=0}^{\infty} (-1)^n \left\{ (2 + 2n - x) \int_0^{t'} \frac{\exp - \left[ \frac{(2+2n-x)^2}{4u} + a^2 u \right]}{u^{3/2}} du \right. \\
 & \left. + (2n + x) \int_0^{t'} \frac{\exp - \left[ \frac{(2n+x)^2}{4u} + a^2 u \right]}{u^{3/2}} du \right\} \quad (19)
 \end{aligned}$$

-Adsorption Insignificant ( $a = 0$ )

$$\begin{aligned}
 C = & \frac{1}{\sqrt{4\pi}} \sum_{n=0}^{\infty} (-1)^n \left\{ (2 + 2n - x) \int_0^{t'} \exp - \left[ \frac{(2+2n-x)^2}{4u} \right] \frac{du}{u^{3/2}} \right. \\
 & \left. + (2n + x) \int_0^{t'} \exp - \left[ \frac{(2n+x)^2}{4u} \right] \frac{du}{u^{3/2}} \right\} \quad (20)
 \end{aligned}$$

### Concentration-History at Metal Substrate Interface ( $x = 1$ )

$$\begin{aligned}
 C = & \sum_{n=0}^{\infty} (-1)^n \left[ e^{(2n+1)a} \operatorname{erfc} \left( \frac{2n+1}{2\sqrt{t'}} + a \sqrt{t'} \right) \right. \\
 & \left. + e^{-(2n+1)a} \operatorname{erfc} \left( \frac{2n+1}{2\sqrt{t'}} - a \sqrt{t'} \right) \right] \quad (21)
 \end{aligned}$$

-Adsorption Insignificant ( $a = 0$ )

$$C = 2 \sum_{n=0}^{\infty} (-1)^n \operatorname{erfc} \left( \frac{2n+1}{2\sqrt{t'}} \right) \quad (22)$$

## Steady State Solutions (t = ∞)

### Concentration Profiles

$$C = \frac{\cosh a(1 - x)}{\cosh a} \quad (23)$$

### Concentration at Substrate

$$C = \operatorname{sech} a \quad (24)$$

## 3.2 Blister Formation and Growth

As discussed in Section 2.2, blister formation and growth occurs as a result of the diffusion of water into the osmotic cell created at the coating-metal interface by impurity ions. Blistering is considered to initiate at the metal substrate interface at weak spots randomly distributed over the substrate surface. These can be rough spots, spots with high impurity ion concentrations or places with incipient adhesion loss. The weakest spots are ones where blisters first initiate. Blister growth occurs when there is sufficient water present in the vicinity of the metal substrate. Osmotically driven diffusion of water through the coating controls the rate of growth. As the blister becomes diluted with water the rate of blister growth slows.

To account for these phenomena several mathematical models are presented here. In the first (developed in subsection 3.2.1), the impurity ions (such as chloride or sulfate) are considered to be concentrated at specific spots on the metal surface where blister initiation occurs. The rest of the surface is presumed to be impurity free. In the second scenario modeled (developed in

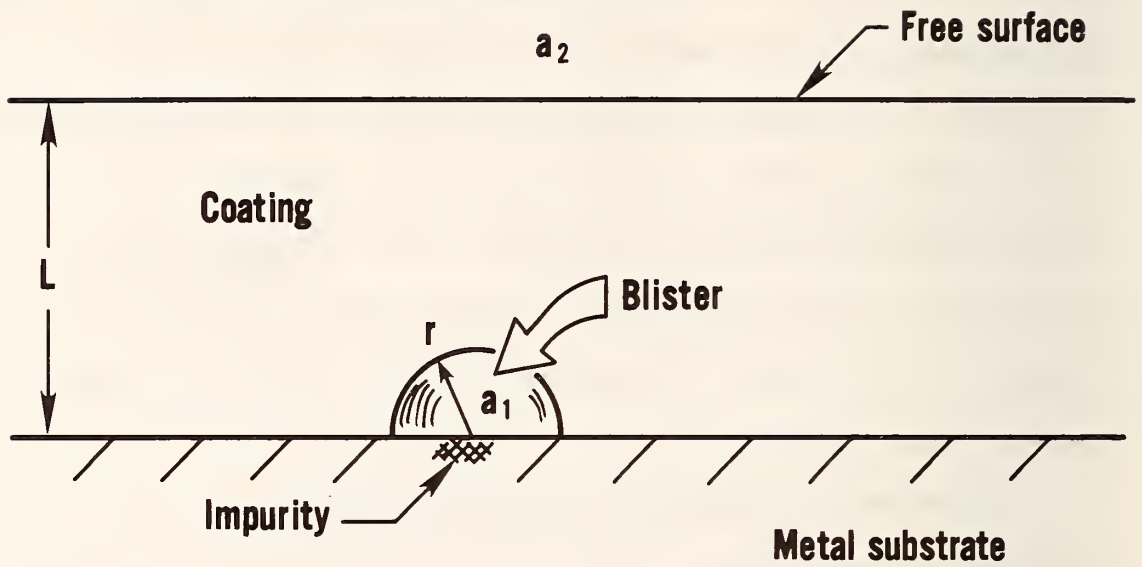
subsection 3.2.2), the impurity ions are considered to be spread uniformly over the whole surface. Blister initiation still takes place over weak spots on the surface, but as the blister ages, new impurity ions are introduced at the periphery. In both models it is presumed that the adhesion loss and the stiffness of the organic coating do not control the rate of blister growth [6, 7]. This means that the effect of the over pressure created by tension in the disbonding film can be neglected. Thus, adhesion loss is considered to be an effect rather than a cause. At later times the osmotic pressure may fall to the point that the tension in the film cannot be overcome. At this point blister growth will stop.

The mathematical models for growth of a blister on a metal substrate are based upon a modified Fick's Law for the diffusion of water which takes the flux of water (N) to be proportional to the product of the effective diffusivity (D) through the coating, the concentration of water in the coating (C) and the gradient of the logarithm of the water activity coefficient ( $d \ln a/dZ$ ) across the coating between the external environment and the interior of the blister [6, 7]. This is expressed mathematically by the relation

$$N = - DC \frac{d \ln a}{dZ} \quad (25)$$

Figure 2 is a schematic representation of a blister within an organic coating. It shows the profile of a single hemispherical blister which has grown to a radius  $r$  within the coating. The water activity coefficient within the blister is  $a_1$ , while that in the external environment above the free surface is denoted by  $a_2$ . The distance  $Z$  is measured normal to the coating from the metal surface. The blister is assumed to remain small relative to the coating thickness.

2A: Concentrated Spot of Impurity



2B: Uniform Distribution of Impurity

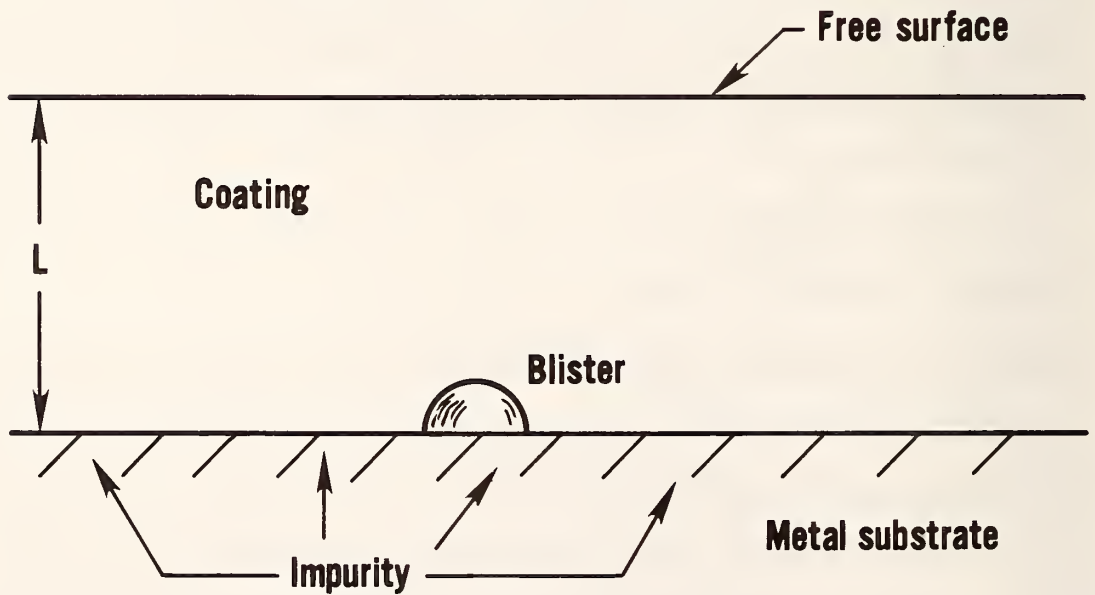


Figure 2: Schematic Representation of a Blister within an Organic Coating

( $r \ll L$ ). This remains true for the initial and middle stages of blister growth. In the later stages of growth, the blister may enlarge to the point where its size approaches or exceeds the initial film thickness  $L$ . For this stage, the models presented in this report will not apply exactly.

The assumptions made in the course of the development of these models are summarized in Table 2. Because of assumption 4 in Table 2 the blistering process is uncoupled with the process of molecular diffusion. Diffusion of water during blistering is driven by the osmotic pressure and not by concentration gradients (Fick's law) as described in the previous section. In effect we are assuming, in this scenario that molecular diffusion is much faster and occurs much sooner than the formation of blisters. By the time the blisters begin to form there is plenty of water in their vicinity. In addition the demand of the few small blisters which form for more water is minimal. This implies that  $C$ , the total concentration of the concentration of water in the coating in the vicinity of the blister, can be treated as a constant.

It can be shown [8, 9] that the gradient of the log of the activity coefficient is proportional to the gradient of the molarity ( $m$ ) of the impurity ion, i.e.,  $(dm/dZ)$ .  $m$  is expressed as moles solute/kg solvent. In this case, in the light of the assumptions given in Table 2, equation (25) can be integrated to give:

$$N = \frac{DC}{\ell} \frac{\bar{M}\phi}{1000} \Delta m \quad (26)$$

TABLE 2: Assumptions of the Mathematical Models for Blister Growth

1. Blister formation does not occur until water is present at the metal - coating interface.
2. Blister does not change shape during growth (presumed hemispherical).
3. Dissolution of impurity ions into the blister from the metal surface does not control growth.
4. Mass transfer of water to the blister surface is driven by osmotic pressure, not by molecular diffusion.
5. Diffusion is unidirectional.
6. Blister size is much less than coating thickness.
7. Desorption of water into the blister from the bottom of the coating is rapid enough that it does not influence growth.
8. Adhesion loss and stiffness of the organic coating do not control blister growth.
9. The coating functions as a semipermeable membrane, allowing water to diffuse osmotically inward but preventing impurity ions from diffusing outward.
10. The molar osmotic coefficient  $\phi$  is constant.
11. Only one impurity (solute) is present.
12. Pigment particles have no effect on the osmosis process.
13. The diffusion coefficient  $D$  (of water in the coating) is constant during osmosis.

where

$\ell$  is the diffusion path length

$\nu$  is the number of ions formed from one molecule of the impurity ion

$\bar{M}$  is the solvent molecular weight (18 for water)

$\phi$  is the molar osmotic coefficient (assumed constant)

The multiplier of  $\Delta m$  on the right hand side of equation (26) is a constant which will be specific to the kind of impurity ion and coating involved.  $\Delta m$  represents the change in molarity of the impurity ion between the blister and the outside of the coating. When the coating is exposed to water containing on impurity ion  $\Delta m$  is equal to  $m$  the molarity of the impurity ion within the blister. The diffusion process can be viewed as being driven by the osmotic pressure difference,  $\Delta\pi$ , which exists between the inside of the blister and the external environment. Thus:

$$\Delta\pi = \frac{RT}{\tilde{V}} \ln \frac{a_2}{a_1} = \left( \frac{RT}{\tilde{V}} \frac{\nu\bar{M}\phi}{1000} \right) \Delta m \quad (27)$$

where

$R$  is the gas constant

$T$  is the absolute temperature

$\tilde{V}$  is the partial molal volume of the solvent (water)

When no impurity ions are present in the external solution, then  $a_2 = 1$  and  $\Delta m = m$ . As the blister becomes diluted with water,  $a_2$  rises and the osmotic pressure within the blister drops. As a result the diffusion process slows.

### 3.2.1. Blister Growth - Concentrated Spots of Impurity

When a concentration of impurity ions such as chloride or sulfate is present at a metal surface together with a sufficient amount of water, then blister initiation and growth occurs. Consider the metal to have a small spot where a high concentration of impurity ions are located. This is shown schematically in Figure 2A.

A water balance equates the increase in mass of the water within the blister to the amount which fluxes through the mantle (curved) surface:

$$\rho \frac{dV}{dt} = \frac{dM}{dt} = \bar{M} S N \quad (28)$$

where

$\rho$  is the density of water within the blister

$V$  is the volume of the blister

$M$  is the mass of water within the blister

$S$  is the surface area of the mantle

With the presumption that the blister retains its shape:

$$\frac{dV}{dt} = S \frac{dr}{dt} \quad (29)$$

where

$r$  is a characteristic dimension of the blister

Substituting equation 29 and equation 26 into equation 28 and rearranging:

$$\frac{dr}{dt} = \left[ \frac{\bar{M}}{\rho} \frac{DC}{l} \frac{\nu M \phi}{1000} \right] \Delta m \quad (30)$$

Equation 30 gives an expression for the rate  $dr/dt$  at which the blister dimension  $r$  increases with time. The volumetric blister growth rate is  $S dr_1/dt$ , while the mass blister growth rate is  $\rho S dr_1/dt$ .

The molarity  $m$  is a function of the amount of salt present at the blister initiation site,  $M_s$ , and the amount of water which has diffused through the blister surface. An electrolyte or salt balance made on the blister yields:

$$\frac{dM_s}{dt} = A r_d \quad (31)$$

where

$A$  is the (flat) area of the blister on the metal surface

$r_d$  is the rate of dissolution based on surface (grams/mm<sup>2</sup>, s)

In general, the dissolution rate  $r_d$  is quite high when compared to the time scale for water diffusion. The impurity ion are concentrated right at the bottom of the blister and they have ready access to the blister interior. The dissolution is effectively complete before much water has had a chance to penetrate the blister. In this case the molality within the blister can be expressed directly as:

$$m = \frac{1000 M_s}{M \bar{M}_s} \quad (32)$$

Substituting equation 32 into equation 30, with  $\Delta m = m$  (no impurity ion in the external phase), and integrating, expressions for the blister radius  $r$ , mantle surface area  $S$  and blister volume  $V$  are obtained as a function of time:

$$r = k_r t^{1/4} \quad (33)$$

$$S = k_s t^{1/2} \quad (34)$$

$$V = k_v t^{3/4} \quad (35)$$

where

$$k_r = \left[ \frac{6}{\pi} \frac{M_s^{DC}}{\ell} \nu \bar{M}^2 \phi \right]^{1/4} \quad (36)$$

$$k_s = 2\pi k_r^2 \quad (37)$$

$$k_v = \frac{2}{3} \pi k_r^3 \quad (38)$$

$k_r$ ,  $k_s$  and  $k_v$  are constants for the radius, surface area, and volume, defined respectively by equations (36), (37) and (38). In the development of these models, the blister was assumed to retain the shape of a hemisphere throughout its growth. The characteristic dimension  $r$  is the radius of the hemisphere. The model can be simply extended to other blister shapes which are surfaces of revolution, such as the segment of a sphere or an ellipsoidal shape.

Equation (35) predicts that the blister mass (or volume) increases as the 0.75 power of time. If the time is doubled the blister volume increases by 68 per cent. The blister radius increases as the 0.25 power of time (equation 33). The blister radius doubles after the time has increased by a factor of 16. These results also predict that the rate of blister growth slows with time, being greater at the beginning when the blister is small and contains a concentrated salt solution, and less later when the solution in the blister has become diluted with water.

Combining equations 27, 32 and 35 an expression can be derived for the osmotic pressure as a function of time:

$$\Delta\pi = k_p M_S^{1/4} t^{-3/4} \quad (39)$$

where

$$k_p = \frac{3}{2\pi\rho} \frac{RT}{\tilde{V}} \left[ \frac{\ell}{6 \bar{MDC}} \right]^{3/4} (\nu\phi)^{1/4} \quad (40)$$

Equation 39 predicts that the osmotic pressure varies the 0.25 of the amount of salt in the blister and reciprocally with the 0.75 power of the time. At time zero the model predicts very large osmotic pressures within the blister. At small times the model predicts very large osmotic pressures within the blister. The molarity, however, cannot exceed the saturation value,  $m^*$ , of the impurity ion in water. This places an upper limit on the osmotic pressure as predicted by equation 27 with  $\Delta m = m^*$ .

The dimension  $\ell$  contained in the equations represents a characteristic diffusion length. In cases where water must be drawn in from the external environment,  $\ell = L$ , the coating thickness. When water is already present as a result of the diffusion process then  $\ell = \delta$ , where  $\delta$  represents a characteristic film thickness ( $\delta < L$ ) for the diffusion process. With no diffusional resistance, water in the vicinity of the blister would pass freely across the mantle surface and blister growth would be quite rapid.

### 3.2.2 Blister Growth - Uniform Distribution of Impurity

The second type of blister growth model considers the impurity ion to be uniformly spread across the surface. This is shown schematically in Figure 2B.

For the growth of a single blister, this differs from the previous model development in one important aspect - as the blister grows, fresh impurity enters through its base. In this case the amount of impurity ion,  $M_s$ , added, to the blister is proportional to the flat or base area,  $A$ , of the blister (equal to  $\pi r^2$  for a hemispherical blister). The greater the area of the peeled blister, the greater is  $M_s$ . Thus

$$M_s = k'A = k'\pi r^2 \quad (41)$$

The proportionality constant  $k'$  in equation 41 is equal to the surface concentration of impurity ions,  $g/mm^2$ .

As in the previous model, this model presumes that the rate of dissolution of impurity ions into the blister is quite rapid compared to the rate of blister growth. Thus, as the blister peels from the surface, the fresh impurity ions exposed on the surface can be considered to immediately transfer into the solution. By substituting equation 41 and equation 32 into equation 30, with  $\Delta m = m$ , and integrating, expressions are obtained for the blister radius, mantle surface area and blister volume as functions of time:

$$r = k'_r t^{1/2} \quad (42)$$

$$S = k'_s t \quad (43)$$

$$V = k'_v t^{3/2} \quad (44)$$

where

$$k'_r = \left[ \frac{3}{2} k' \frac{\bar{M}}{\bar{M}_s} \frac{DC}{C^2 \ell} v \phi \right]^{1/2} \quad (45)$$

$$k'_s = 2\pi k'_r{}^2 \quad (46)$$

$$k'_v = \frac{2}{3} \pi k'_r{}^3 \quad (47)$$

$k'_r$ ,  $k'_s$  and  $k'_v$ , are the constants in equations (42), (43) and (44), defined, respectively by equations (45), (46) and (47).

An expression for the osmotic pressure within a blister growing over a surface containing a uniform amount of impurity is obtained by combining equations 27, 32, 41, 42, 45 and 47:

$$\Delta\pi = k'_p t^{-1/2} \quad (48)$$

where

$$k'_p = 1000 \left[ \frac{\frac{3}{2} k'_v \nu \phi}{\bar{M} \bar{M}_s} \frac{\ell}{DC} \right]^{1/2} \quad (49)$$

The specific values of the osmotic pressure depend on the value of the osmotic rate constants,  $k'_p$  given by equation 49.

### 3.3 Corrosion Phenomena

Corrosion is possible and, after sufficient time probable, whenever water, oxygen and an electrolyte are in proximity to a metal surface. Because the metal is at a higher free energy level than the corrosion products, there is a driving force for corrosion. The potential for corrosion can be evaluated by considering the difference in potential between the half-cell reactions which occur at the anodic and cathodic sites on the metal surface. For any

given coating-metal system, the tendency to corrode varies with the temperature, and concentrations of water, oxygen and electrolyte in the vicinity of the metal. Higher values of any of these variables can act to accelerate the corrosion process. When concentrations of one of the chemical species are low, e.g. oxygen, corrosion rates depend on the rate at which it is transported to the cathodic site. Since oxygen permeation controls the observed corrosion rate, it can then be considered to be the rate-limiting step. In a similar fashion, water permeation would be rate-controlling if the concentration of water at the corrosion site were low. This could result from: a) low relative humidity outside the coating, b) low affinity of the coating for water (low  $C_{i0}$ ), c) high affinity of the pigment for water (high  $k_a$ ), d) slow diffusion of water through a relatively thick coating.

The electrolyte itself would control observed rates whenever its concentration in the water solution were low. This would result from low initial concentrations of impurity ions on the metal surface (clean surface) and dilution of the electrolyte by water within a blister because of osmotic flow. Since the corrosion reactions themselves can generate electrolytes (e.g., hydroxyl ions), the process can be self-accelerating or autocatalytic, with more and more ions being released into solution. This, in turn, may raise the ionic strength within the blister leading to the incursion of more water. The enlarging cathode area associated with the growing blister can accelerate the corrosion even more, both because of the larger area and the differential aeration which occurs where oxygen has easier access at the periphery of the blister.

### 3.3.1 Potential Difference Model

The greater the potential difference between the anode and cathode, the greater will be the driving force for corrosion. As the corrosion reactions proceed, the driving force diminishes because of the build-up of reaction products in the vicinity of the electrode surfaces. Thus the driving force for corrosion is the potential difference between the anode and the cathode. The initial value of the driving force is determined from the thermodynamic potentials of the half cell reactions (refer to Section 2.3). The existence of this potential causes electron flow and corrosion proceeds. As the potential of the cathode,  $E_C$ , drifts towards that of the anode,  $E_A$ , and vice versa, polarization occurs. Polarization was modeled in terms of the potential difference  $\delta$  between the anode and the cathode, where  $\delta = E_A - E_C$ . Thus the cathode potential rises (and the anode potential falls) at a rate which is proportional to this difference in potential.

Mathematically, this is expressed as

$$\frac{dE_C}{dt} = k_C \delta \quad (50)$$

$$\frac{-dE_A}{dt} = k_A \delta \quad (51)$$

$k_C$  and  $k_A$  are unknown polarization rate constants for the cathode and anode, respectively. Their units are reciprocal time,  $s^{-1}$ . They vary with temperature and anode and cathode surface area. Thus:

$$k_A = k_{A\infty} S_A \exp [ -L_A/RT ] \quad (52)$$

$$k_C = k_{C\infty} S_C \exp [ -L_C/RT ] \quad (53)$$

where

$S_A, S_C$  are the anode (A) and cathode (C) surface areas

$L_A, L_C$  are the activation energies for the anode and cathode

$R$  is the gas constant

and

$k_{A\infty}, k_{C\infty}$  are specific rate constants (based on area) for the anode and cathode.

Equations 52 and 53 are based on the presumption that the rate constants follow an Arrhenius - law type temperature dependence, and, in fact,  $k_{A\infty}$  and  $k_{C\infty}$  are analogous to Arrhenius frequency factors. When the temperature and surface areas of the anode and cathode are constant, and the electrode has a uniform potential across it, both  $k_A$  and  $k_C$  are fixed and equations 50 and 51 can be solved analytically to give<sup>+</sup>:

$$\frac{E_C}{E_{OC}} = \left[ \frac{k_A + k_C \frac{E_{OA}}{E_{OC}}}{k_A + k_C} \right] + \frac{k_C}{k_A + k_C} \left( 1 - \frac{E_{OA}}{E_{OC}} \right) e^{-(k_A + k_C) t} \quad (54)$$

$$\frac{E_A}{E_{OC}} = \left[ \frac{k_A + k_C \frac{E_{OA}}{E_{OC}}}{k_A + k_C} \right] + \frac{k_A}{k_A + k_C} \left( \frac{E_{OA}}{E_{OC}} - 1 \right) e^{-(k_A + k_C) t} \quad (55)$$

$$\delta = (E_{OA} - E_{OC}) e^{-(k_A + k_C) t} \quad (56)$$

---

<sup>+</sup> The complete derivation of these equations is given in Appendix B.1.

$E_{OA}$  and  $E_{OC}$  are the initial potentials of the anode and the cathode, respectively.  $(E_{OA} - E_{OC})$  is equal to initial potential difference, which can be found from the thermodynamic half cell potentials.

Equations 54 and 55 predict that the anode potential decreases and the cathode potential rises at ever decreasing rates towards a common final potential  $E_f$  given by:

$$E_f = \frac{k_A E_{OC} + k_C E_{OA}}{k_A + k_C} \quad (57)$$

Equation 56 gives the driving force  $\delta$  for the polarization process. It decreases exponentially with time. After a suitably long time polarization is complete,  $\delta \rightarrow 0$ , and both anode and cathode have the potential given by equation 57.

### 3.3.2 Equivalent Circuit Model

An alternative model can be developed in which the polarization process can be modeled in terms of an equivalent electrical circuit. Figure 3 shows a schematic of the circuit. The anode and the cathode are taken to be at the opposite end of a charged capacitor  $C_a$  having an initial thermodynamic potential  $\delta_0 = E_{OA} - E_{OC}$ .

As with the potential difference model developed in the previous section, this model is based on a voltage difference  $\delta$  between half cell reactions. This falls with time and eventually reaches some steady state value. The existence of a potential causes electron flow through the solution and polarization proceeds. The driving force is represented in the model by a charged capacitor. Initially the capacitor is fully charged. As shown in figure 3,

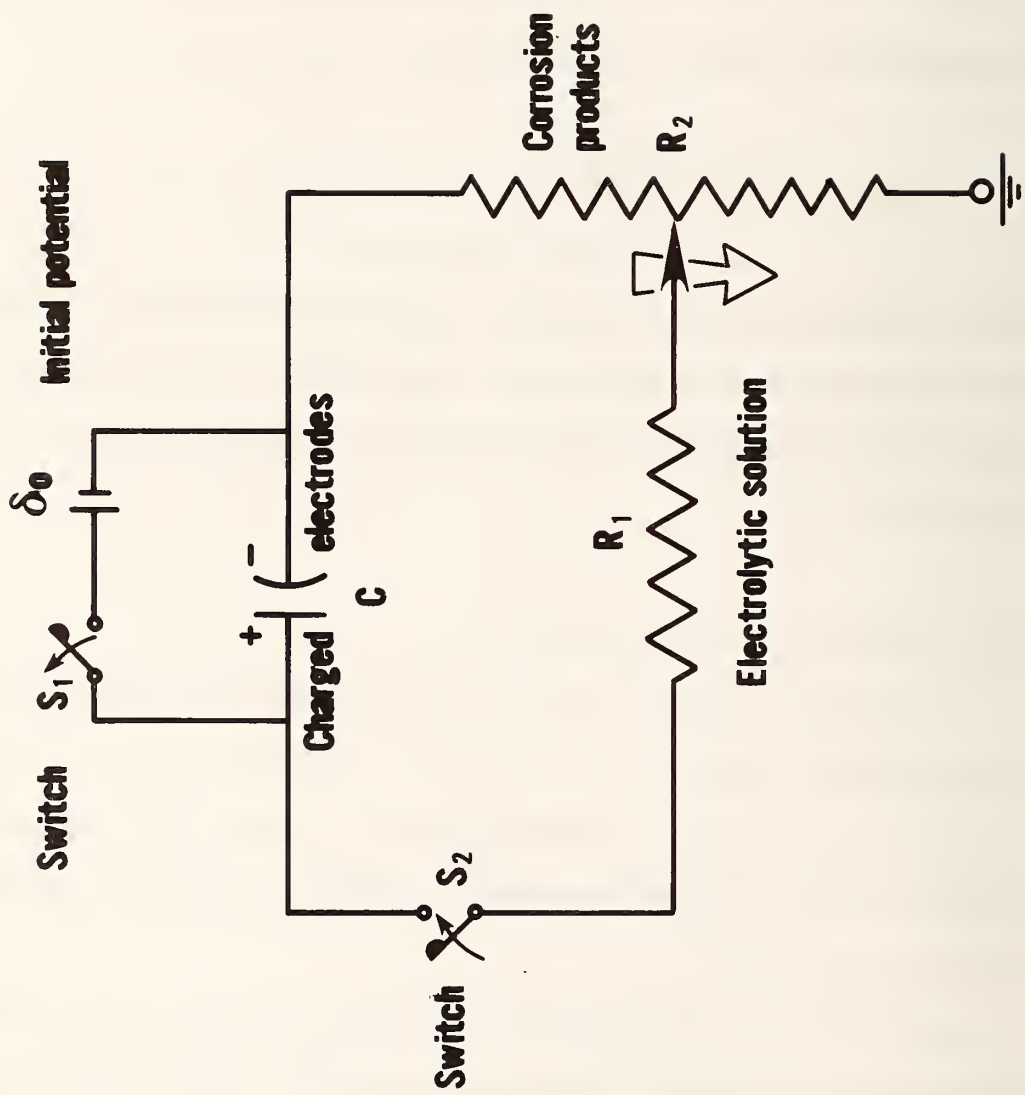


Figure 3: Equivalent Electrical Circuit for Polarization

at time zero the switch  $S_1$  is opened, the switch  $S_2$  is closed, and the circuit is completed. The capacitor then slowly discharges through the resistances.

The electrolyte serves as a charge carrier for the electron flow. But the presence of the electrolytic solution contributes to the overall resistance of the electrical circuit. The resistance  $R_1$  will remain the same as long as the composition and conductivity of the solution remains the same. At the beginning of the polarization process, before the products of corrosion have accumulated, this is likely to be true. Also at later times when the corrosion products have come to a pseudo-equilibrium with the electrolyte solution,  $R_1$  would also tend to be constant. In between,  $R_1$  would decrease from its old level towards a new level. The decrease in resistance is caused by an increase in ionic conductivity as product ions, particularly  $\text{OH}^-$  and  $\text{Fe}^{++}$  are released into the solution. When the concentration of these ions reach the solubility limit, solid reaction products precipitate from solution and the conductivity becomes constant again.

The initial potential decreases because of the electron transfer or flow of current. The initial current decreases both because of the decreasing potential, and the increasing resistance  $R_2$  (refer to figure 3), attributable to the corrosion products. The products can form an adsorbed film of ions or gases on the cathode surface, or a solid layer of corrosion products such as  $\text{Fe}(\text{OH})_3$  or  $\text{Fe}_2\text{O}_3$  can deposit on the surface. In either case, the resistance increases with time, although film formation would be more rapid than product layer formation.

With film formation either of two mechanisms can operate:

- a) a monolayer of ions or gases can adsorb on the electrode surface (Langmuir adsorption mechanism).
- b) an electrical double layer can form in the vicinity of the surface.

For mechanism (a), ions (or gases) adsorb on active sites located on the metal surface at a rate which is proportional to the product of the number of unoccupied sites with the concentration of ions in the bulk solution. They desorb at a rate proportional to the number of occupied sites. These assumptions are analogous to those of the classical Langmuir theory for the physical adsorption of gases. The electrical resistance of the adsorbed ions ( $R_2$ ) will be proportional to the fraction of the total surface which is occupied. Based on the Langmuir theory, it can be shown that

$$R_2 = (R_2)_u [1 - e^{-\alpha t}] \quad (58)$$

where

$(R_2)_u$  is the ultimate or final resistance

and

$\alpha$  is the rate constant for film formation by Langmuir adsorption

The development of equation 58 presumes that the concentration of adsorbing ions in the conducting fluid medium does not change with time. This is reasonable considering the relatively small number of ions which can generally supply monolayer coverage to a surface. Equation 58 predicts that  $R_2$  increases linearly with time at the beginning of the corrosion process when the surface has only a small coverage of adsorbed ions. At later times, when the surface

---

<sup>+</sup> The complete derivation of equation 58, including the determinations of the values of  $(R_2)_u$  and  $\alpha$  in terms of Langmuir theory, is presented in Appendix B.2.2.

is nearly covered, the resistance approaches a constant value. If the rate of increase is high, corresponding to a large value of the constant  $\alpha$ , then monolayer coverage is rapid and  $R_2$  is constant during most of the corrosion process.

An electrical double layer can also form next to the electrode surface as a result of the electric field in the interface region between the metal surface and the solution [10]. Water, which has a large dipole moment, can form an ionic cloud near the metal surface. The water dipoles next to the metal surface orient themselves depending on the charge on the metal. This inner layer of water molecules is known as the "hydration sheath." The second layer out from the surface contains saturated ions and is known as the "outer Helmholtz plane." Together the hydration sheath and Helmholtz plane comprise an electrical double layer. The formation of a double layer increases the resistance to the transfer of electrical charge, and specifically,  $R_2$ . At present, the precise way in which  $R_2$  varies with the charge and composition of the electrical double layer has not been determined.

Solid corrosion products such as  $\text{Fe}_2\text{O}_3$  or  $\text{Fe}(\text{OH})_2$  can deposit on the surface. These, too, will increase the resistance  $R_2$  and cut down on the charge transfer. If the products accumulate uniformly over the surface of the metal, the resistance increases in direct proportion to the thickness of the corrosion layer. Thus:

$$R_2 = \beta \ell = \gamma \int_0^t i dt = \gamma (Q_0 - Q) = \gamma C_a (\delta_0 - \delta) \quad (59)$$

where

$\ell$  is the thickness of the corrosion products

$\beta, \gamma$  are empirical constants of proportionality

$i$  is the current

$Q$  is the charge

$Q_0$  is the initial charge

The thickness  $\ell$  can only be measured accurately if a tarnish layer accumulates, but it can be implied from the theory developed here.

Equation 59 expresses the fact that the total amount of corrosion product laid down, by Faraday's Law, are proportional to the total corrosion current which has flowed until time  $t$ , i.e.  $\int_0^t i dt$ . This in turn will be equal to the change in charge,  $(Q_0 - Q)$  or  $C_a (\delta_0 - \delta)$ . Thus, the resistance at any time is proportional to the degree of polarization.

Referring again to Figure 3, it is possible to derive expressions for the charge  $Q$ , the current  $i$ , and the voltage drop  $\delta$ , provided the resistance of the electrolytic solution,  $R_1$ , and the resistance of the corrosion products,  $R_2$ , are known as functions of system variables.

Applying Kirchoff's Second Law (the algebraic sum of the potential differences around any closed loop is zero) to the electrical circuit shown in figure 3:

$$i (R_1 + R_2) + \frac{1}{C_a} \int_0^t i dt = 0 \quad (60)$$

since

$$i = \frac{dQ}{dt} \quad (61)$$

Equation 60 can be rewritten as

$$(R_1 + R_2) \frac{dQ}{dt} + \frac{Q}{C_a} = 0 \quad (62)$$

with the initial condition that

$$Q_0 = C_a \delta_0 \quad (63)$$

With assumptions made about  $R_1$  and  $R_2$ , these circuit equations were solved to give the charge,  $Q$ , current,  $i$ , and potential difference,  $\delta$ , as functions of time. In all of the developments, both  $C_a$ , the capacitance of the charged electrodes, and  $R_1$ , the electrolyte resistance, were taken as constants.

Three different sub-models were used for  $R_2$ , the resistance of the corrosion products. These included:

- (a) a constant value of  $R_2$
- (b)  $R_2$  based on film formation by Langmuir adsorption (equation 58)
- (c)  $R_2$  based on the uniform accumulation of a layer of corrosion products (equation 59)

Solutions to each of these sub-models for  $Q$ ,  $i$  and  $\delta$  are summarized here. They are based on the circuit-model equations, 60, 61, 62 and 63. Derivations are supplied in Appendix B.2.

When  $R_2$  is constant, sub-model (a) predicts that:

$$\frac{Q}{Q_0} = \frac{i}{i_0} = \frac{\delta}{\delta_0} = \exp \left[ \frac{-t}{(R_1 + R_2) C_a} \right] = \exp (-t/\tau) \quad (64)$$

where

$$i_o = \frac{\delta_o}{R_1 + R_2} \quad (65)$$

and

$$\tau = (R_1 + R_2)C_a \quad (66)$$

Equation 64 predicts that the relative charge, current and potential difference all fall exponentially at the same rate.  $\tau = (R_1 + R_2)C_a$  represents a time constant for this process. In general,  $\tau$  will be an unknown model constant since  $C_a$  is unknown. The initial current  $i_o$  is calculated using equation 65, from the initial potential,  $\delta_o$ , and total circuit resistance.

When  $R_2$  is based on film formation by Langmuir adsorption (sub-model (b)) the corresponding formulas for  $Q$ ,  $\delta$ , and  $i$  are:

$$\frac{Q}{Q_o} = \frac{\delta}{\delta_o} = \left[ \left(1 + \frac{R_u}{R_1}\right) e^{\alpha t} - \frac{R_u}{R_1} \right] e^{-\frac{t}{\alpha \tau_u}} \quad (67)$$

$$\frac{i}{i_o} = \frac{\left[ \left(1 + \frac{R_u}{R_1}\right) e^{\alpha t} - \frac{R_u}{R_1} \right] e^{-\frac{t}{\alpha \tau_u}}}{\left[1 + \frac{R_u}{R_1}\right] (1 - e^{-\alpha t})} \quad (68)$$

where

$$\tau_u = C_a (R_1 + R_u) \quad (69)$$

$\tau_u$  is a system time constant based on the final resistance ( $R_1 + R_u$ ) which corresponds to equilibrium monolayer coverage of the electrode surface.

Equation 67 predicts that the relative charge and potential difference should both fall in the same manner. Equation 68 gives an analogous expres-

sion for the current. The initial current  $i_o$  is equal to  $\delta_o/R_1$  in this case, since  $R_2$  is initially zero. A comparison of equations 67 and 68 shows that:

$$\frac{\delta}{\delta_o} = \frac{i}{i_o} \left(1 + \frac{R_2}{R_1}\right) \quad (70)$$

Since  $R_2$  increases with time equation 66 predicts that the relative current,  $i/i_o$ , falls faster than the potential difference ratio,  $\frac{\delta}{\delta_o}$ . At large values of the constant  $\alpha$ :

$$\frac{Q}{Q_o} = \frac{\delta}{\delta_o} = \left(1 + \frac{R_u}{R_1}\right)^{-t/\tau} \quad (71)$$

while

$$\frac{i}{i_o} = \left(1 + \frac{R_u}{R_1}\right)^{-(1+\frac{t}{\tau})} \quad (72)$$

Physically large values of the constant  $\alpha$  corresponds to the rapid attainment of equilibrium of the adsorbing species with the metal surface.

When  $R_2$  is based on the accumulation of a layer of solid corrosion products, the corresponding formulas for  $Q$ ,  $\delta$ , and  $i$  are:

$$\frac{Q}{Q_o} = \frac{\delta}{\delta_o} = \exp \left[ \frac{C_a \gamma Q_o (1-Q/Q_o) - t}{C_a (R_1 + \gamma Q_o)} \right] \quad (73)$$

$$\frac{i}{i_o} = \frac{Q}{C_A [R_1 + \gamma Q_o - \gamma \frac{Q}{Q_o}]} \quad (74)$$

Equation 73 is transcendental in  $Q/Q_0$ , and must be solved numerically for specific values of model parameters. Once  $Q/Q_0$  is known, the current ratio  $i/i_0$  can be found from equation 74.

#### 4. DISCUSSION OF RESULTS

##### 4.1 Water and Oxygen Permeability

Equations 14 through 24 present expressions for the water and oxygen concentrations within the coating and at the metal substrate as a function of time. The equations for the concentration are expressed in terms of dimensionless variables and parameters: dimensionless concentration,  $C = C_i/C_{i0}$ , dimensionless depth,  $x = z/L$ , dimensionless time,  $t' = tD_i/\epsilon L^2$ , and dimensionless parameter,  $a$ , defined by equation 15. It is advantageous to express the model in terms of dimensionless groups since in effect, all possible cases can be condensed into a single mathematical form.

Even though the models have the same mathematical structure, they predict that each species penetrates the film at different rates. This is because specific model parameters will differ for each penetrant. These parameters are  $C_{i0}$ , the concentration of penetrant dissolved at the top of the coating,  $D_i$ , the effective diffusion coefficient of penetrant through the coating and  $k_{ai}$ , the adsorption coefficient of the penetrant on the surface of the pigment particles.

For a given coating (fixed  $L$  and  $\epsilon$ ), the actual values of  $C_{i0}$ ,  $D_i$  and  $k_{ai}$  will determine the concentration of the penetrant at the metal substrate as a function of time. Each penetrant's concentration rises towards its final or steady-state value. The rate of rise depends on the value of the model parameters.

The concentrations at the coating-substrate interface depend on  $t'$  and the degree to which pigment particles are effective in removing water and/or oxygen. Permeation to the surface becomes important at times  $t$  when the dimensionless time ( $t'$ ) is of the order of unity ( $t' \sim 1$ ). It is important to emphasize that it is  $t'$  which affects the rate at which steady-state is attained rather than the absolute time  $t$ .

For  $t' < 1$  the short time model solutions (equations 19, 20, 21 and 22) should be used. For  $t' > 1$  the long time model solutions (equations 14, 15, 16, 17 and 18) should be used. For dimensionless times  $t' \sim 1$ , either set of solutions produce equivalent answers, with a similar number of terms needed for convergence in the infinite series. At such times, the penetrant concentrations in the coating will have risen to within a significant fraction of their final or steady-state values. Thus the protective performance of the film will be enhanced if  $D_i$  is small,  $L$  is large and  $\epsilon$  is small. The most sensitive of these parameters is the film thickness,  $L$ . If  $L$  is doubled it takes four times as long for the penetrant to reach a given fraction of its final concentration. This is one of the reasons why the use of multiple coats of paint is preferred. From this single viewpoint, using five coats of paint is over thirty times as effective as a single coat.

In addition to dimensionless time  $t'$ , concentrations at the coating-substrate interface also depend on the affinity of the penetrants for the pigment particles. A quantitative measure of this effect is provided by the dimensionless parameter  $a$ , as defined by equation 15.

$$a = L \left[ \frac{6k}{d} \frac{a_i}{D_i} \left( \frac{1-\epsilon}{\epsilon} \right) \right]^{1/2} = L \left[ \frac{6k}{d} \frac{a_i}{D_i} (p/v) \frac{\rho_v}{\rho_p} \right]^{1/2} \quad (15)$$

The higher the value of the parameter  $a$ , the greater is the retention of the penetrant within the organic coating. Water and oxygen have different values of  $a$ , mainly because of the different chemical attraction they have for the pigment particles when dissolved in the vehicle. The parameter  $a$  is a function of pigment loading,  $(p/v)(\rho_v/\rho_p)$ , pigment particle diameter,  $d$ , diffusivity,  $D_i$ , affinity of the pigment particle for the penetrant, as measured by the adsorption coefficient  $k_{ai}$ , and coating thickness  $L$ .  $a$  can take on any positive value, including zero. Realistically,  $a$  can be zero if no pigment is used (as in varnishes) or if the pigment has no affinity for the penetrant, i.e.  $k_{ai} = 0$ . For example,  $a = 0$  if oxygen absorbed in the coating does not adsorb on the surface of titanium dioxide ( $TiO_2$ ) pigment particles.

In order to keep the concentrations of the penetrants small at the metal surface and, thus minimize the potential for corrosion, it is best to design a coating system which has a high value of the parameter  $a$ . According to equation 15 this will occur with a suitable combination of the following factors:

1. lots of small sized pigment particles ( $p/v$  high,  $d$  low)
2. retarded diffusion through the coating ( $D$  low)
3. rapid adsorption onto pigment particles ( $k_{ai}$  high)
4. thick coating ( $L$  large)

The parameter  $a$  is most sensitive to this last factor.  $a$  varies in direct proportion to coating thickness, doubling the thickness doubles the value of  $a$ . This is in contrast with the other parameters which vary directly or inversely with the square root, which is a less sensitive function. All of the factors listed act to retain the penetrant within the coating, not allow-

ing it to reach the metal surface. Two additional factors will also act to keep penetrant concentrations low at the metal substrate:

5. low solubility of the penetrant into the vehicle (low  $C_{i0}$ )
6. short contact times (low  $t'$ )

Thus, even in the worst possible case, where  $a = 0$ , it is still possible to have low concentrations at the metal surface if the solubility of the penetrant into the vehicle is low, for the concentration at the surface may never exceed this value. Also, the concentrations at the metal surface do not start to reach an appreciable fraction of their final or steady-state values until the dimensionless contact time  $t'$  is approximately unity. Thus, the surface concentration relative to its final value remains low until time  $\theta$ , where the characteristic time  $\theta$  is given by:

$$\theta = \epsilon L^2 / D_i \quad (75)$$

For a typical film with  $L = 0.1$  mm,  $D_i = 0.5 \times 10^{-6}$  mm<sup>2</sup>/s (an estimate) and  $\epsilon = 0.5$ , this leads to  $\theta = 1000$ s. Typical service lives of most organic coatings are many orders of magnitude greater than this. This implies that steady state will be attained in a matter of hours (at least for this value of the diffusivity). Thus short contact times may not be an important contributing factor. However, for lower values of the diffusivity (say  $D_i \sim 10^{-10}$  mm<sup>2</sup>/s, which would be typical of solid-state diffusivities) the contact time would become an important factor [11, 12].

Examining the diffusion process in terms of the overall protective function of the coating, both water and oxygen must be present in concentrations which

are sufficient to initiate and accelerate corrosion. The steady state concentrations of oxygen and water at the metal surface are given by equation 24 as

$$C_i = C_{i0} \operatorname{sech} a_i \quad (24)$$

Whether or not corrosion will actually occur will depend on the temperature, pH, nature of the metal and electrolyte and the electrochemical potentials of the half-cell reactions. In some instances corrosion will not occur regardless of the oxygen concentration because it is thermodynamically unfavorable or favors the formation of a passive oxide film. Pourbaix diagrams of potential vs pH are convenient ways to summarize such information [13]. In some regions it is possible to go from a condition where corrosion is not possible to one where it is, by simply increasing the oxygen concentration. At the point where this occurs the specific concentration is denoted as  $C_{O_2,c}$ . Whether or not corrosion will actually occur cannot be determined a priori but this concentration represents a threshold above which corrosion is possible. In addition as the oxygen concentration is raised the probability that corrosion will occur becomes more likely. Since the concentrations at the substrate rise with time at suitably long times the limit  $C_{O_2,c}$  may be exceeded for a given coating and environment. Thus the possibility for corrosion will exist when  $C_{O_2,c}$  is less than the steady state value. The absence of corrosion is indicated by:

$$C_{i0} \operatorname{sech} a_i < C_{ic} \quad (76)$$

where

$$i = O_2$$

To insure that corrosion will not occur, equation 76 need only be valid for oxygen or water. For such a system, corrosion is prevented if  $a$  can be raised, or  $C_o$  lowered, to the point where the inequality is obeyed for oxygen. For an existing coating system,  $a$  can be raised most conveniently by applying extra layers of coating, while  $C_o$  can be lowered most conveniently by lowering the concentration of penetrant in the external phase. In laboratory situations the partial pressure of oxygen can be lowered, e.g., by dilution with nitrogen, or in aqueous systems by bubbling nitrogen through the solution. Coatings exposed to the atmosphere will have the partial pressure fixed at 0.21 atm. In terms of the design of a coating system, the model predicts that better protection will be afforded if:

1. a large fraction of pigment is used in the formulation
2. smaller particles are used
3. a denser, thicker coating is applied
4. the coating is made oxygen and water repellent

Using the model, the exact quantitative effort of each of these factors can be assessed.

#### 4.2 Blister Formation and Growth

In section 3.2 two mathematical models were developed for the growth of water-filled blisters at the metal substrate under the coating. Both models were based on diffusion and osmotic theory and had a single adjustable constant, the osmotic rate constant. Equations were given for the radius, mantle surface area, and volume of a hemispherical blister as a function of time.

In the first model (refer to section 3.2.1), blister growth was considered to occur over concentrated spots of impurity located at the point of

blister initiation. No new impurity ions come into the blister as it grew. This model was mathematically expressed by equations 33 through 40, with the osmotic pressure relationships given by equations 39 and 40. In the second model (refer to section 3.2.2), blister growth was considered to occur over an unclean surface which contained a uniform distribution of impurity. As the blister grew, fresh impurity entered through its base. This model is mathematically expressed by equations 42 through 49, with the osmotic pressure relationships given by equations 48 and 49.

Both models have the same mathematical form - the radius, surface area and blister volume all vary directly as the time raised to various fractional powers. Also, for both models, the blister volume varies as the cube of the blister radius, while the mantle and flat surface areas both vary with the square of the radius. Comparing the model solutions for concentrated impurity distribution (equations 33, 34 and 35), with those found for uniform salt distribution (equations 42, 43 and 44), shows that the blister size increases more rapidly with the uniform salt distribution. Blister size will double when the time has increased by a factor of 1.6, compared to a factor of 2.5 for concentrated salt distribution. As time proceeds, the rate of blister growth actually increases (as  $\sqrt{t}$ ). This is unlike the concentrated salt distribution case where a decrease in volumetric growth rate with time is predicted.

Of course a true comparison of the absolute (rather than relative) sizes of the blisters for the two models needs to be made based on the release of equivalent amounts of salt into the blister. In many cases the salt spot on the surface is present as a small patch. Surface diffusion gives a more or less uniform salt concentration over the patch. It is likely that the center

of such a spot has a slightly higher salt concentration so that blister initiation is favorable there. The model developed for uniform salt distribution is applicable until the blister has grown to the size of the patch, after which the model for concentrated salt distribution applies. Data of blister volume vs time would show a sharp change in slope at this time.

Equations 39 and 48 present expressions for the osmotic pressure within blisters for the concentrated impurity and uniform impurity models, respectively. For both models, the osmotic pressure is predicted to fall with time as the blister solution becomes diluted with water. The models incorrectly predict an infinite osmotic pressure at time zero. In actuality, the highest osmotic pressure would be that corresponding to the saturation value of the impurity salt in water at the temperature of the system. Comparing equation 39 with 48 shows that the osmotic pressure falls off most rapidly when the salt is initially concentrated within the blister rather than being uniformly spread across the metal. This will be true for both changes in the absolute value of the osmotic pressure,  $d(\Delta\pi)$ , and the relative value,  $d(\Delta\pi)/\Delta\pi$ . Thus from equations 39 and 48 it can be shown that:

$$\frac{-d(\Delta\pi)}{\Delta\pi} = \frac{1}{2t} \quad (77)$$

and

$$\frac{-d(\Delta\pi)}{\Delta\pi} = \frac{3}{4t} \quad (78)$$

for the uniform and concentrated salt models, respectively. Comparing equation 78 to equation 77 shows that the relative change in the osmotic pressure  $-d(\Delta\pi/\Delta\pi)$  is greater when the salt is concentrated, since any given time  $t$ , equation 78 predicts the relative rate of fall of osmotic pressure will be larger.

Of course when all the salt is concentrated within the blister, the initial osmotic pressure is much greater than when the salt is uniformly distributed. In this case the osmotic pressure has further to fall. For uniform salt distribution, osmotic pressures do not fall as fast because the concentration of fresh salt is being added at the periphery of the blister. As with blister growth rates, it is best to compare osmotic pressures based on the availability to the blister of the same total amount of salt.

At later times the osmotic pressure can fall to the point where the disbonding tension in the film cannot be overcome and blister growth will cease. Blister initiation does not occur when the surface is relatively clean, when the adhesion of the coating to the substrate is good or where water has not penetrated to the surface. The osmotic pressure developed is insufficient to destroy the adhesion, and the blister does not form.

Blister initiation can also be prevented by reversing the concentration gradient. Thus if a concentrated salt solution is kept in the external solution outside the coating, water may be drawn from the coating. This is the principle which makes it possible to store acids and concentrated salts in painted vessels made of metals which would normally corrode. This helps prevent the initiation of blisters and can collapse existing blisters, although wrinkling of the coating may be observed. The models developed in this report for blister growth can easily be modified to treat blister collapse.

It is important to understand the extent to which the blister initiation and growth processes are coupled with the absorption and diffusion processes discussed in the previous section. The interaction of these processes depends on both time and distance scales. Thus, if blister initiation and growth is

slow compared to the time taken for water to diffuse to the metal-coating interface, then blister formation is more likely and initial blister growth more rapid because of the proximity of the water to the surface. The diffusion path for water will then be much less than the thickness of the coating and diffusion times considerably shortened. If, on the other hand, blister growth is inherently faster than the diffusion rate of water, then water will need to be drawn into the blister all the way from the surface of the coating. The observed rate of blister growth will then be controlled by the absorption and diffusion rates of water within the coating.

For a surface containing only a few small blisters, the amount of water drawn to the coating-metal interface will not depend on the number of blisters. This is because the total demand of these blisters for water is small compared to the amount of water which can be absorbed by the vehicle or adsorbed by the pigment. Thus, even though water diffusion has a pronounced effect on blister growth, the reverse is not true. However, as the number of blisters per unit area of coating (number density of blisters) increases, a point will be reached where a significant fraction of the water which reaches the metal-coating interface will be brought there as a result of osmotic effects.

For systems with multiple blisters, the number density of blisters is an important parameter. The models developed here for single blisters must be extended in order to treat blister clusters. Additional factors to consider include:

1. the possibility of blister impingement and coalescence with other blisters
2. diffusion of water along the surface in addition to normal to the surface
3. different blisters initiating at different times and growing at different rates

This last factor is possible if the surface has a distribution of weak spots having different adhesive strengths or if there is a non-uniform concentration of impurity ions on the metal.

#### 4.3 Corrosion Phenomena

In section 4.2 two mathematical models were developed for the corrosion phenomena which occur in organic coating systems. Both models treated the polarization which occurs when an electrical potential is dissipated in an electrochemical cell. These models are the potential difference model (PDM) and the equivalent circuit model (ECM). The (ECM) itself has three separate submodels, one based on a constant value of the resistance of the corrosion products, one based on Langmuir adsorption (or film formation) of the corrosion products on the cathode surface, and one based on a uniform accumulation of layers of corrosion products. Both the (DCM) and (ECM) models consider that an electrochemical cell having an anode and cathode is formed beneath the coating. The models are not specific to any particular corroding system. They presume surface uniformity and do not account for changes in size or location of the anode or cathode surfaces.

In the potential difference model (PDM) (presented in section 3.3.1) the driving force for polarization is the potential difference between the anode and the cathode. The potential difference between cathode and anode was found to decrease exponentially with time (equation 56), while the cathode and anode potentials themselves (equations 54 and 55), exponentially approached a final common potential (given by equation 57). The models contain two unknown polarization rate constants, which vary directly with electrode surface area and follow an Arrhenius temperature dependency.

The equivalent circuit models (ECM), as presented in section 3.3.2, are based upon the dissipation of the initial potential across two series resistances, one corresponding to the resistance of the electrolytic solution ( $R_1$ ), and the second corresponding to the resistance of the corrosion products ( $R_2$ ). Solutions are presented for the charge, current and potential difference of the circuit. When  $R_2$  is constant the potential difference predicted across the circuit, (equation 60), has the same mathematical form as that for the (PDM), equation 56. In fact a comparison of the two equations shows that:

$$\tau = (R_1 + R_2)C_a \sim \frac{1}{k_A + k_B} \quad (79)$$

Thus the circuit time constant  $(R_1 + R_2)C_a$  is analogous to the reciprocal of the sum of the polarization rate constants.

For the other (ECM) submodels for  $R_2$ , the potential difference also decreases with time, but the mathematical analogy to the (PDM) is no longer valid.

For all (ECM) models the circuit current and charge also decreased with time. When  $R_2$  is a constant, the charge, current and potential difference all decrease exponentially from their initial values in the same way (refer to equation 60). For the film formation and uniform product accumulation submodels, the potential and charge decrease together, but the current falls faster because of the increase of  $R_2$  with time.

The models developed in this report can be used to fit polarization data for two dissimilar metals immersed in a fluid media containing ionized acid, base or salt. Because polarization is fairly rapid (scale of minutes) compared to the time scale of other corrosion phenomena, such as pitting or precipitation

of corrosion products, it can be considered to be an important phenomenon during the earlier stages of the corrosion process. The corrosion reactions themselves produce charge by generating electrons at the anode as the metal is consumed. This is not accounted for in the models. In fact, the polarization models predict a decrease in charge with time.

In addition, the increase in solute or electrolyte concentration with time due to the accumulation of ions of corrosion product has not been modeled. In the models this would result in a decrease in  $R_1$ , the resistance of the electrolytic solution or conducting medium. When ions in the electrolyte "soup" reach critical concentrations determined by the ionic field and the solubility products, precipitation occurs. Precipitation acts as a sink for ions so that the resistance of the electrolyte may approach a constant value. Refinements in the model should take these factors into account.

For any given coating - metal system the tendency to corrode varies with the temperature and concentrations of water, oxygen and electrolyte in the vicinity of the metal. Higher values of any of these variables act to accelerate the corrosion process. When concentrations of one of the chemical species are low, e.g. oxygen, corrosion rates depend on the rate at which it is transported to the cathodic site. Oxygen permeation through the film can then be considered to be the rate-limiting step since it controls the observed corrosion rate. In a similar fashion, water permeation would be rate-controlling if the concentration of water in the vicinity of the corrosion site were low. This could result from: a) low relative humidity outside the coating, b) low affinity of the coating for water (low  $C_{i0}$ ), c) high affinity of the pigment for water (high  $k_{ia}$ ) d) slow diffusion of water through a relatively thick coating. The solute or electrolyte itself would control rates whenever its

concentration in the water solution were low. This can result from low initial concentrations of impurity ions on the metal surface (clean surface), or dilution of the electrolyte by water within a blister because of osmotic flow. Since the corrosion reactions themselves can generate electrolytes (e.g., hydroxyl ions) the process can be autocatalytic, with more and more ions being released into solution. This, in turn, can raise the ionic strength within the blister leading to the incursion of more water. The enlarging cathode area associated with the growing blister can accelerate the corrosion even more, both because of its larger area and the differential aeration which occurs at the periphery of the blister where oxygen has easier access.

As discussed in the previous section, blister formation and growth will depend on the location and amount of water which has penetrated the coating. In the same way, the accumulation of corrosion products can alter the osmotic pressure within the blister. This, in turn, can affect the rate at which water is drawn to the blister. Decreases in ion concentrations raise the circuit resistance and cut down on the rate of corrosion.

In summary, the overall corrosion process is complex. The separate mathematical models developed in this paper for permeation of water and oxygen, for the growth of blisters and for the polarization of electrode surfaces were all modeled independently of one another, as if these processes were uncoupled. Yet both diffusion and osmotic pressure can indirectly influence the amount of corrosion which can occur beneath a blistered coating. Future modeling and experimental efforts should be directed at a more complete understanding of the coupling which occurs between these phenomena.

## 5. SUMMARY AND CONCLUSIONS

Mathematical models were developed for conceptual models describing the main phenomena which occur when corrosion occurs beneath an organic coating. The potential for corrosion exists when oxygen, water and ionic impurities are present together in the vicinity of the metal substrate. This situation is likely to occur in blisters, which are water filled cavities located at the metal-coating surface. Blisters grow because of osmosis of water from the coating. Their rate of growth depends on their size and the concentration of impurity ions within them and outside the coating, as well as the location and distribution of water within the coating. The penetrants water and oxygen both enter the coating by absorption and then pass through the coating by diffusion. Not all of the penetrant may reach the metal surface because of adsorption on the surface of the pigment particles. All of these processes are a function of the nature of the coating system and temperature. The rates of absorption, diffusion and adsorption differ for water and oxygen.

Within blisters, corrosion reactions can initiate if sufficient dissolved oxygen is present. For iron-based metals oxidation at the anode produces ferrous ions, while reduction at the cathode consumes water and oxygen to form hydroxyl ions. Electrons generated at the anode flow through the metal to the cathode where they are accepted by the cathodic reaction. Pitting of the anode can occur, while corrosion products generally form in the vicinity of the cathode. This can cause polarization of the cathode surface, as can the formation of adsorbed films of gases and ions or the formation of electrical double layers.

Mathematical models were developed and solved for:

- a) the permeation of water and oxygen through the coating (absorption, diffusion and adsorption)
- b) the growth of blisters on the metal substrate
- c) polarization of the anode and cathode surfaces

Permeation models were based on the flux laws and conservation laws for the diffusing species. At the outside coating surface the water and oxygen were assumed to absorb by Henry's Law. Adsorption of penetrants onto the pigment surface was assumed to occur at a rate proportional to the local concentration and the concentration of pigment particles. A volume balance related the porosity of the coating (volume fraction vehicle) to the pigment to vehicle weight ratio. Diffusion was modeled based on Fick's Law. For both oxygen and water the separate rate laws established for adsorption, diffusion and absorption were incorporated into the overall conservation equations. This formulation resulted in two linear partial differential equations; one for oxygen and one for water. Both equations had the same mathematical form. The dependent variable was the concentration and the independent variables were the depth into the coating and time. Parameters in the model included the pigment to vehicle ratio, the pigment particle size, the diffusivity of the penetrant through the coating ( $D_i$ ) its solubility in the coating ( $C_{i0}$ ) and the adsorption coefficient of the penetrant onto the pigment particles ( $k_i$ ). Since  $C_{i0}$ ,  $D_i$  and  $k_i$  have different values for water and oxygen, the rates of absorption, diffusion and adsorption differ.

Model solutions for concentration as a function of coating depth and time were expressed in terms of dimensionless variables and parameters. Both short and long time solutions to the mathematical model were presented, as were

steady state profiles and concentrations at the metal-coating surface. The model predicted that the permeation of water and oxygen would be inhibited and, thus, the potential for corrosion lessened, with a suitable combination of:

1. lots of small sized pigment particles
2. retarded diffusion through the coating
3. rapid adsorption onto pigment particles
4. thick (or multiple) coating(s)
5. low solubility of penetrant into vehicle (water and oxygen repellancy)
6. short dimensionless contact times

Of all of these factors the model was found to be most sensitive to the coating thickness  $L$ . Increases in  $L$  gave much lower concentrations of water and oxygen at the metal surface as well as lower dimensionless contact times. The protective function of the coating is greatly enhanced if membrane thickness is raised. It was shown that for short contact times, given by  $\epsilon L^2/D_i$ , penetration to the surface is unlikely to initiate blister growth and subsequent corrosion.

Corrosion will not occur unless oxygen and a conducting solution are present at a metal surface. Even then, corrosion is not possible unless it is thermodynamically favored, as indicated, for example, by conditions of oxygen concentration, pH, temperature and electromotive potential which place it in the active region of the appropriate Pourbaix diagram. As a result of exposure of a coating to an outside oxygen environment, concentrations at a potential corrosion site increase. Corrosion can then become thermodynamically favored as passage from a passive to an active region occurs. At this point a critical

value of oxygen concentration,  $C_{ic}$ , is reached. It was established, that even if a steady state were attained, oxygen might not be present at the metal surface in this concentration. Mathematically this was expressed by  $C_{io}$  such  $a_i < C_{ic}$ , where  $a$  is a dimensionless parameter which is a measure of the retention of oxygen by the coating. Under these conditions corrosion cannot occur although the converse does not hold.

Blister growth was considered to occur either over concentrated spots of impurity located at the point of blister initiation or over a surface containing a uniform concentration of impurity. The solutions to both models had similar mathematical forms: the blister radius, surface area, volume and osmotic pressure were all found to vary directly as fractional powers of the time. Blister volume varied as  $t^{0.75}$  for concentrated spots of impurity and as  $t^{1.5}$  for a uniform distribution of impurity. The relative value of the osmotic pressure was predicted to fall more rapidly for the concentrated distribution of impurity, due to the rapid dilution of the blister with water. For a uniform distribution of impurity the osmotic pressure does not fall as fast because fresh salt is continually being added at the periphery of the blister. The coupling between blister formation and the permeation of water was discussed in terms of the time and distance scales characteristic of each process.

Two mathematical models were developed for the corrosion phenomena occurring in organic coatings. These were the potential difference model and the equivalent circuit model. The models treated the polarization occurring when an electrical potential is dissipated in an electrochemical cell. In the polarization model, the driving force was the potential difference between the anode and the cathode. Model solutions predicted that the potential difference

decreases exponentially with time so that both anode and cathode potentials slowly approach a common final potential.

In the second model, corrosion was modeled in terms of an equivalent electrical circuit. Polarization rates were taken to be functions of the electromotive force and the circuit resistance. The potential between the anodic and cathodic sites within the corrosion cell was considered to be dissipated across several series resistances. These included the resistance of the electrolyte and the resistance of the corrosion products. Corrosion product resistance was attributable to the formation of product layers next to the cathode surface. The resistance of the electrolyte was taken as a constant while the resistance of the corrosion products ( $R_2$ ) was modeled using several different submodels. This included a constant value of  $R_2$ , one based on Langmuir adsorption (or film formation) of corrosion products and one based on uniform accumulation of layers of corrosion products.

All of the models predicted that the potential between electrodes, the charge and the current decrease with time. The equivalent circuit submodel for constant  $R_2$  was shown to be analogous to the potential difference submodel. For the film formation model the potential and charge decreased together but the current fell faster because of the increase of  $R_2$  with time. Refinements in the model were suggested which would take into account the nature of the corrosion reactions, the charge they generate and the increase in electrolyte concentration with time.

The coupling between the corrosion process, the blistering process, and the permeation process was discussed. The coupling is complex and only the separate processes were modeled in this paper. Future modeling and experimental efforts will be directed at elucidating a fuller understanding of the nature of the coupling.

## 6. NOMENCLATURE

a	adsorption - diffusion constant, equation (15); activity coefficient, equation (25)
$a_1$	water activity coefficient within blister
$a_2$	water activity coefficient in external solution
A	flat area of blister on metal surface
b	defined by $(2n + 2 - x)$
C	dimensionless concentration, $C_i/C_{i0}$ ; concentration of water, equation (25)
$C_a$	capacitance of charged electrodes
$C_i$	concentration of component i within coating
$C_{i0}$	concentration of component i inside coating surface
$C_{ic}$	critical value of $C_i$ , equation (76)
d	diameter of pigment particles
D	diffusion coefficient or diffusivity
$D_i$	diffusion coefficient or diffusivity of component i
$D_i^*$	molecular (or Knudsen) diffusivity
$E_A, E_C$	potential of anode and cathode, respectively
$E_{OA}, E_{OC}$	initial potential of anode and cathode, respectively
$\bar{E}_A, \bar{E}_C$	Laplace transform of $E_A$ and $E_C$ , respectively
$E_f$	final potential, equation (57)
$H_i$	Henry's Law constant for component i
i	current
$i_0$	initial value of current

$k_{ai}$	adsorption rate constant for component $i$
$k_A, k_C$	anodic and cathode polarization rate constants, equations (51) and (50), respectively
$k_{A\infty}, k_{C\infty}$	specific rate constants for the anode and cathode, respectively
$k_d$	desorption rate constant
$k_p$	rate constant for osmotic pressure, equation (39)
$k_r, k_s, k_v$	rate constants for radius, area and volume, equations (36), (37) and (38), respectively
$k'$	proportionality constant, equation (41)
$k_r, k_s, k_v$	rate constants; equations (45), (46), (47) respectively
$\ell$	diffusion path length; thickness of corrosion products
$L$	thickness of coating or film
$L_A, L_C$	activation energias for anode and cathode, respectively
$m$	molarity of impurity ion
$m^*$	saturation value of $m$
$M$	mass of water in the blister
$M_s$	amount of salt present at blister initiation site
$\bar{M}$	solvent molecular weight
$\bar{M}_s$	salt molecular weight
$n$	number density of particles; summation index
$N$	diffusive flux; number of occupied sites
$N_i$	diffusive flux of species $i$
$N_t$	total number of sites
$(p/v)$	volume ratio, pigment to vehicle
$p_{io}$	partial pressure of component $i$ in external phase
$Q$	charge
$Q_0$	initial value of $Q$

$r$	characteristic dimension of blister
$r_d$	rate of dissolution based on surface
$r_{is}$	rate of adsorption of penetrant $i$ per particle
$R$	gas constant
$R_1$	resistance of electrolyte solution
$R_2$	resistance of corrosion products
$(R_2)_u$	ultimate or final value of $R_2$
$s$	Laplace transform variable
$S$	surface area of blister mantle
$S_A, S_C$	surface areas of anode and cathode, respectively
$S_1, S_2$	switches, figure 3
$t$	time
$t'$	dimensionless time
$T$	absolute temperature
$u$	transformation relation, equation (A-5)
$\bar{u}$	Laplace transform of $u$
$V$	volume of blister
$\bar{V}$	solvent partial modal volume
$x$	dimensionless distance, $Z/L$
$Z$	depth into coating measured from free surface

#### GREEK LETTERS

$\alpha$	rate constant for film formation by Langmuir adsorption, equation (58)
$\beta, \gamma$	constants of proportionality, equation (59)
$\nabla$	gradient
$\delta$	characteristic film thickness for diffusion; potential difference ( $E_A - E_C$ )

$\delta_o$	initial value of potential difference
$\epsilon$	porosity of coating (volume fraction vehicle)
$\Delta\pi$	change in osmotic pressure
$\nu$	number of ions formed from one molecule of impurity ion
$\phi$	molar osmotic coefficient
$\rho$	density of water within blister
$\rho_p$	density of a pigment particle
$\rho_v$	density of the vehicle (binder)
$\sigma$	constriction factor (equation 6)
$\tau$	tortuosity factor (equation 6); time constant (equation 66)
$\tau_u$	time constant based on final resistance; equation (69)
$\theta$	fraction of occupied sites, $N/N_t$
$\theta_e$	equilibrium surface coverage, equation (B-17)

## 7. REFERENCES

1. Perera, D. Y., and Van den Eynde, D., "Alternation in Properties of Organic Coatings for Buildings Due to the Leaching Process," Durability of Building Materials and Components, ASTM STP691, 698-710 (1980).
2. Kumms, C. A., "Physical Chemical Models for Organic Protective Coatings," Journal of Coatings Technology 52 (664), 40-53 (1980).
3. Ritter, J. J., and Kruger, J., "Studies on the Sub-Coating Environment of Coated Iron Using Qualitative Ellipsometric and Electrochemical Techniques," Surface Sci. 96, (1980).
4. Peterson, E., Chemical Reaction Analysis, Prentice-Hall, New York, 1965.
5. Bruggeman, D. A., Ann. Physik 24, 636 (1935).
6. van der Meer - Lerk, L. A., and Heertjes, P. M., "Blistering of Varnish Films on Substrates Induced by Salts," J. Oil Col. Chem. Assoc. 58, 79-84 (1975).
7. van der Meer - Lerk, L. A., and Heertjes, P. M., "Mathematical Model of Growth of Blisters in Varnish Films on Different Substrates," J. Oil Col. Chem. Assoc. 62, 256-263 (1979).
8. Robinson, J. M., and Stokes, R. H., Electrolyte Solutions, 2nd edition, Butterworth, London, 1970.
9. Harned, H. S., and Owen, B., The Physical Chemistry of Electrolytic Solutions, 3rd edition, ACS Monograph No. 137, Reinhold Press, New York, 1958.
10. Bockris, J. O'M., and Reddy A. K. N., Modern Electrochemistry, Volume 2, Plenum Press, New York, 1973.
11. Crank, J., and Park G. S., Diffusion in Polymers, Academic Press, New York, 1968.
12. Artamonova, R. V., et.al., "Internal Stresses and Water Diffusion in Polymers," (trans.) Vysokomol. soyed. A12, No. 2 (1970), pp. 336-342.
13. Uhlig, H. H., Corrosion and Corrosion Control, 2nd edition, John Wiley & Sons, Inc., New York, 1971.
14. Thirsk, H. R., and Harrison, J. A., A Guide to the Study of Electrode Kinetics, Academic Press, London, 1972.
15. Satterfield, C. N., Heterogeneous Catalysis in Practice, McGraw-Hill, New York, 35-37, 1980.

APPENDIX A  
 SOLUTION TO MATHEMATICAL MODEL FOR  
 DIFFUSION OF WATER AND OXYGEN  
 THROUGH ORGANIC COATINGS

In this Appendix the analytical solutions to the mathematical models developed in Section 3.1 are derived. These are the models which describe the concentration of water and oxygen within the coating. The solutions are summarized by equation number in Table 1 of Section 3.2, and are presented as equations (14) through (24) in the text which follows. The solutions are classified by time region of validity: short time, long time, or steady-state; by phenomena: with and without adsorption; and by location: within the bulk of the coating and at the substrate-metal interface.

Equations (9) gives the partial differential equation which governs the concentration profile of water and oxygen  $C_i (Z,t)$  within the organic coating:

$$\epsilon \frac{\partial C_i}{\partial t} = D_i \frac{\partial^2 C_i}{\partial Z^2} - \frac{6 k_{ai}}{d} (1 - \epsilon) C_i \quad (9)$$

Equations (10), (11), and (12) give the boundary and initial conditions:

$$C_i (0,t) = C_{i0} \quad (10)$$

$$\frac{\partial C_i}{\partial Z} (L,t) = 0 \quad (11)$$

$$C_i (Z,0) = 0 \quad (12)$$

The solution to Equation (9), subject to the conditions (10), (11), and (12), gives the concentration profiles  $C_i(Z,t)$  within the coating.

Introducing the dimensionless variables  $x = z/L$ ,  $C = C_i/C_{i0}$  and  $t' = tD_i/\epsilon L^2$  (equation 13), equations (9), (10), (11) and (12) become equations (A-1), (A-2), (A-3), and (A-4), respectively:

$$\frac{\partial C}{\partial t'} = \frac{\partial^2 C}{\partial x^2} - a^2 C \quad (A-1)$$

$$C(0, t') = 1 \quad (A-2)$$

$$\frac{\partial C}{\partial x}(1, t') = 0 \quad (A-3)$$

$$C(x, 0) = 0 \quad (A-4)$$

The solution to Equation (A-1) subject to the conditions (A-2), (A-3) and (A-4) gives the dimensionless concentration profile  $C(x, t')$  within the coating.

The parameter  $a$  is defined by Equation (15):

$$a = L \left[ \frac{6k_{ai}}{dD} \frac{(1-\epsilon)}{\epsilon} \right]^{1/2} = L \left[ \frac{6k_{ai}}{dD} (p/v) (\rho_v/\rho_p) \right]^{1/2} \quad (15)$$

$a$  is a dimensionless adsorption-diffusion constant which is fixed for any coating system and environment. The paint films are presumed to contain a uniform distribution of spherical pigment particles of diameter  $d$ . The assumption of particle sphericity is not critical to model development because the concept of an equivalent sphere (one having the same surface area as the non-

spherical particle) can be employed. The porosity  $\epsilon$  is the volume fraction of the coating occupied by the vehicle. Equation (2) is a volume balance made on the coating:

$$\epsilon = \frac{1}{1 + (p/v) (\rho_v/\rho_p)} \quad (2)$$

Equation (2) is the basis for the equivalence of the second equality in Equation (15).

#### A.1 Long Time Model Solutions

The long time model solutions developed in this section are ones which converge fastest at longer times. When the solution involves an infinite number of terms fewer and fewer of these terms will be needed for convergence as time increases.

By making the variable transformation from  $C$  (old dependent variable) to  $u$  (new dependent variable) using the transformation relation:

$$u = Ce^{a^2 t'} \quad (A-5)$$

equations (A-1), (A-2), (A-3) and (A-4) become equations (A-6), (A-7), (A-8) and (A-9), respectively.

$$\frac{\partial u}{\partial t'} = \frac{\partial^2 u}{\partial x^2} \quad (A-6)$$

$$u(0, t') = e^{a^2 t'} \quad (A-7)$$

$$\frac{\partial u}{\partial x}(1, t') = 0 \quad (\text{A-8})$$

$$u(x, 0) = 0 \quad (\text{A-9})$$

The boundary value problem expressed by these equations can either be solved by either Fourier Series or Laplace Transform methods. The Laplace Transform method is more general in that it can handle both long and short time solutions. Thus it is employed here.

Taking the Laplace Transform of Equation (A-6) with respect to the time variable  $t'$ , the transformed equations become:

$$\frac{d^2 \bar{u}}{dx^2} - s\bar{u} = 0 \quad (\text{A-10})$$

$$\bar{u}(0, s) = 1/s - a^2 \quad (\text{A-11})$$

$$\frac{d\bar{u}}{dx}(1, s) = 0 \quad (\text{A-12})$$

Here  $\bar{u}$  is the transformed value of  $u$ . It is a function of  $x$  and  $s$ , where  $s$  is the complex variable or transformed value of  $t'$ .

By standard methods the solution to Equation (A-10) is:

$$\bar{u}(x, s) = A \sinh \sqrt{s} (1 - x) + B \cosh \sqrt{s} (1 - x) \quad (\text{A-13})$$

Evaluating the integration constants  $A$  and  $B$  using conditions (A-11) and (A-12):

$$\bar{u}(x,s) = \frac{\cosh \sqrt{s} (1-x)}{(s-a^2) \cosh \sqrt{s}} \quad (\text{A-14})$$

The inverse transform of Equation (A-14) can be found by evaluating it as the product of two functions,  $f(s) = 1/s-a^2$  and  $g(s) = \cosh \sqrt{s} (1-x)/\cosh \sqrt{s}$ , and using the convolution theorem for the product of two functions of  $s$ :

$$u(x,t') = L^{-1} [f(s) \cdot g(s)] = \int_0^{t'} F(t'-u) \cdot G(u) du \quad (\text{A-15})$$

Here the operator  $L^{-1}$  indicates the inverse transform of the convolution product  $f(s)$  times  $g(s)$ .

In Equation (A-15),  $F(t'-u) = e^{a^2(t'-u)}$ .  $G(t')$  can be evaluated from  $g(s)$  using the method of poles and residues or from the Heavisides inversion theorem:

$$G(t') = \pi \sum_{n=1}^{\infty} (-1)^{n-1} (2n-1) \exp \left[ -\frac{(2n-1)^2}{4} \pi^2 t' \right] \cos \left[ \left( \frac{2n-1}{2} \right) \pi (1-x) \right] \quad (\text{A-16})$$

Performing the convolution integral in Equation (A-15) upon these functions:

$$u(x,t) = \pi \sum_{n=1}^{\infty} \frac{(-1)^{n+1} (2n-1) \cos \left[ \frac{(1-x)(2n-1)\pi}{2} \right]}{a^2 + \frac{(2n-1)^2 \pi^2}{4}} e^{a^2 t'} - e^{-\frac{(2n-1)^2 \pi^2}{4} t'} \quad (\text{A-17})$$

Expressed in terms of the original dimensionless concentration  $C$ , equation (A-17) takes the form:

$$C(x, t') = \frac{\cosh a(1-x)}{\cosh a} - \pi \sum_{n=1}^{\infty} \frac{(-1)^{n+1} (2n-1) e^{-[a^2 + (2n-1)^2 \frac{\pi^2}{4}] t'}}{a^2 + (2n-1)^2 \frac{\pi^2}{4}} \cos [(1-x)(2n-1)\pi/2] \quad (A-18)$$

Equation (A-18) is equation (14) of the main text of this paper.

This equation governs the concentration of water and oxygen within the coating as a function of both time and position. Concentrations of the penetrants water and oxygen, although they both are predicted to follow equation (A-8), will differ because of their different values for the parameters  $C_0$ ,  $D$ , and  $k_a$ . This, in turn, through equation (15), will give different values of the dimensionless parameter  $a$ . The additional parameters  $d$ ,  $(p/v)$ ,  $L$  and  $(\rho_v/\rho_p)$  will vary with the nature of the coating system. Thus different coatings will have different values of  $C_0$  and  $a$  and would be expected to perform differently from one another in terms of their resistance to the penetration and permeation of water and oxygen.

As mentioned previously, Equation (A-18) will take fewer terms to converge at longer values of time and for this reason it is referred to as a "long-time" solution.

At very long dimensionless times  $t'$ , Equation (A-18) reduces to:

$$C(x, \infty) = \frac{\cosh a(1-x)}{\cosh a} \quad (A-19)$$

Equation (A-19) is Equation (23) of the main text of this paper. It governs the steady-state concentration profiles within the coating. This relation can also be derived more fundamentally by setting the accumulation term  $\partial C/\partial t'$  equal to zero in equation (A-9) and solving the resulting ordinary differential equation.

The way in which the dimensionless concentration  $C$  varies with dimensionless time  $t'$  at the metal substrate interface ( $x=1$ ) is given by:

$$C(1, t') = \operatorname{sech} a - \sum_{n=1}^{\infty} \frac{(-1)^{n+1} (2n-1) \exp \left[ - \left[ a^2 + (2n-1)^2 \frac{\pi^2}{4} \right] t' \right]}{a^2 + (2n-1)^2 \frac{\pi^2}{4}} \quad (\text{A-20})$$

Equation (A-20) is equation (17) of the main text. It governs the concentration-history at the metal substrate interface ( $x=1$ ).

The steady-state concentration at the metal-substrate interface is given by:

$$C(1, \infty) = \operatorname{sech} a \quad (\text{A-21})$$

which is also equation (24).

In addition to the sub-models given here for the concentrations at the metal substrate interface ( $x=1$ ), other sub-models can be derived for the case where adsorption is insignificant ( $a=0$ ). Note that small  $a$  (tending towards zero) is favored by small  $L$ ,  $k_a$ ,  $(p/v)$  and  $(\rho_v/\rho_p)$  and large  $d$  or  $D$ . If  $k_a = 0$  then there is absolutely no affinity of the penetrant for the pigment particles and  $a$  will be identically zero. For  $a = 0$ , equation (A-18) becomes:

$$C(x, t') = 1 - \frac{4}{\pi} \sum_{n=1}^{\infty} (-1)^{n+1} \exp \left[ - (2n-1)^2 \frac{\pi^2}{4} t' \right] \cos \left[ (2n-1) \frac{\pi}{2} (1-x) \right] \quad (\text{A-22})$$

Equation (A-22) is the same as equation (16).

Concentration histories at the metal substrate interface  $C(1, t')$  in the presence of insignificant adsorption ( $a = 0$ ) are given by:

$$C(1, t') = 1 - \frac{4}{\pi} \sum_{n=1}^{\infty} \frac{(-1)^{n+1}}{2n-1} \exp \left[ -\frac{(2n-1)^2 \pi^2}{4} t' \right] \quad (\text{A-23})$$

which agrees with equation (18) of the text.

## A.2 Short Time Model Solutions

The short time model solutions developed in this section are ones which converge fastest at shorter dimensionless times  $t'$ . When the solution involves an infinite number of terms, fewer and fewer of these terms will be needed for convergence as time decreases. The short and long time solutions should give the same numerical result since they are equivalent mathematically. At intermediate dimensionless times ( $t' \sim 1$ ) the series at short and long times should be equally efficient in converging to a common numerical answer.

The solutions which converge fastest at the shortest dimensionless times  $t'$  can also be obtained by Laplace Transform methods equation (A-14) can be rewritten as:

$$\bar{u}(x, s) = \frac{e^{-x\sqrt{s}} + e^{-(2-x)\sqrt{s}}}{(s-a^2)(1 + e^{-2\sqrt{s}})} \quad (\text{A-24})$$

By dividing the numerator of Equation (A-24) by the term  $(1 + e^{-2\sqrt{s}})$ :

$$\bar{u}(x, s) = \sum_{n=0}^{\infty} \frac{(-1)^n \exp[-(2n+x)\sqrt{s}]}{s-a^2} + \frac{(-1)^n \exp[-(2n+2-x)\sqrt{s}]}{s-a^2} \quad (\text{A-25})$$

The two separate terms in equation (A-25), both of which are under the summation sign, can be evaluated using the convolution integral, equation (A-15).

Letting  $f(s) = 1/(s-a)^2$  and  $g(s) = \exp[-b\sqrt{s}]$ , where  $b = (2n + x)$  in the first summation and  $b = (2n + 2 - x)$  in the second summation, then it follows that,  $F(t') = e^{a^2 t}$  and  $G(t') = \frac{b}{2\sqrt{\pi t'}^3} \exp\left[-\frac{b^2}{4t'}\right]$ . Invoking the convolution

integral, equation (A-15), equation (A-5) and equation (A-25) are inverted to give:

$$C(x, t') = \frac{1}{\sqrt{4\pi}} \sum_{n=0}^{\infty} (-1)^n (2n + 2 - x) \int_0^{t'} \frac{\exp\left[-\frac{(2n + 2 - x)^2}{4u} + a^2 u\right]}{u^{3/2}} du$$

$$+ (-1)^n (2n + x) \int_0^{t'} \frac{\exp\left[-\frac{(2n + x)^2}{4u} + a^2 u\right]}{u^{3/2}} du \quad (A-26)$$

In equation (A-26) both terms are under the summation sign. Equation (A-26) is identical to equation (19). It is the general short time solution. Equation (A-26) is a general solution to the diffusion problem governing the dimensionless concentrations  $C$  within the organic coating as a function of dimensionless distance  $x$  and time  $t'$ . It is mathematically equivalent to equation (A-18), or equation (14). Together equations (A-18) and (A-26) comprise a useful matched set of equations, one good for determining concentration profiles at long dimensionless times, (A-18), and one good for determining concentration profiles at short dimensionless times, (A-26).

The way in which the dimensionless concentration  $C$  varies with dimensionless time  $t'$  at the metal substrate interface ( $x=1$ ) is given by:

$$C(1, t') = \frac{1}{\sqrt{\pi}} \sum_{n=0}^{\infty} (-1)^n (2n + 1) \int_0^{t'} \frac{\exp\left[-\frac{(2n + 1)^2}{4u} + a^2 u\right]}{u^{3/2}} du \quad (A-27)$$

Equation (A-27) can be shown to be identical to equation (21). It governs the concentration-history at the metal substrate interface ( $x=1$ ) and is the short time solution which complements equation (A-20), the solution which converges fastest at long times.

When adsorption of the diffusing species is insignificant,  $a = 0$ . Under this condition the general short time solution, equation (A-26) reduces to:

$$C(x, t') = \frac{1}{\sqrt{4\pi}} \sum_{n=0}^{\infty} (-1)^n (2n + 2 - x) \int_0^{t'} \exp - \frac{(2n + 2 - x)^2}{4u} \frac{du}{u^{3/2}} \\ + (-1)^n (2n + x) \int_0^{t'} \exp - \frac{(2n + x)^2}{4u} \frac{du}{u^{3/2}} \quad (A-28)$$

In equation (A-28) both terms are under the summation sign. Equation (A-28) is identical to equation (20). It governs the dimensionless concentration profiles in the coating in the absence of significant adsorption onto the pigment particles. Since it converges fastest at short dimensionless times it complements equation (A-22), which converges quickest at long dimensionless times.

Concentration histories at the metal substrate interface  $C(1, t')$  in the presence of insignificant adsorption ( $a = 0$ ) are given by:

$$C(1, t') = 2 \sum_{n=0}^{\infty} (-1)^n \operatorname{erfc} \left( \frac{2n + 1}{2\sqrt{t}} \right) \quad (A-29)$$

The dimensionless concentration at the metal substrate interface  $C(1, t')$  is expressed in terms of an infinite series of complementary error functions.

Equation (A-28) is identical to equation (22). It converges fastest at short dimensionless times and thus complements equation (A-23), the solution which converges most rapidly at long dimensionless times.

## APPENDIX B

### SOLUTION TO THE MATHEMATICAL MODEL FOR CORROSION PHENOMENA BENEATH AN ORGANIC COATING

In this Appendix the analytical solutions to the mathematical models developed in Section 3.3 are derived. These are models which describe the polarization which occurs when an electrical potential is dissipated in an electrochemical cell. The models are the potential difference model (PDM) and the equivalent circuit model (ECM). The equivalent circuit model has three submodels depending on the nature of the resistance offered by the corrosion products: constant resistance, Langmuir adsorption or film formation and uniform accumulation of solid products.

#### B.1 Potential Difference Model

In this model the driving force for corrosion is the difference in potential  $\delta$  between the anode and cathode potentials,  $E_A$  and  $E_C$ , respectively.

Thus

$$\frac{dE_C}{dt} = k_C (E_A - E_C) = k_C \delta \quad (B-1)$$
$$E_C(0) = E_{OC}$$

and

$$\frac{-dE_A}{dt} = k_A (E_A - E_C) = k_A \delta \quad (B-2)$$
$$E_A(0) = E_{OA}$$

The initial conditions for equations (B-1) and (B-2) are  $E_{OC}$  and  $E_{OA}$ , respectively. If the temperature within the electrochemical cell does not change then equations (52) and (53) predict that the rate constant  $k_A$  and  $k_C$  will remain constant. Under this condition equations (B-1) and (B-2) form a coupled set of linear first order differential equations whose solution can be obtained by the method of Laplace Transforms.

Taking the Laplace Transform of equations (B-1) and (B-2) and rearranging:

$$\bar{E}_C (s + k_C) = E_{OC} + k_C \bar{E}_A \quad (B-3)$$

and

$$\bar{E}_A (s + k_A) = E_{OA} + k_A \bar{E}_C \quad (B-4)$$

Solving equations (B-3) and (B-4) simultaneously for the transformed potentials,  $\bar{E}_C(s)$  and  $\bar{E}_A(s)$ :

$$\bar{E}_C = \frac{s + k_A}{s (s + k_A + k_C)} \left[ E_{OC} + \frac{k_C E_{OA}}{s + k_A} \right] \quad (B-5)$$

and

$$\bar{E}_A = \frac{E_{OC}}{s + k_A} + \frac{k_A E_{OC} (s + k_A + k_C + E_{OC}/E_{OC})}{s (s + k_A) (s + k_A + k_C)} \quad (B-6)$$

Taking the inverse transform of equations (B-5) and (B-6)

$$\frac{E_C}{E_{OC}} = \frac{k_A + k_C \frac{E_{OA}}{E_{OC}}}{k_A + k_C} + \frac{k_C}{k_A + k_C} \left( 1 - \frac{E_{OA}}{E_{OC}} \right) e^{-(k_A + k_C) t} \quad (\text{B-7})$$

and

$$\frac{E_A}{E_{OC}} = \frac{k_A + k_C \frac{E_{OA}}{E_{OC}}}{k_A + k_C} - \frac{k_A}{k_A + k_C} \left( 1 - \frac{E_{OA}}{E_{OC}} \right) e^{-(k_A + k_C) t} \quad (\text{B-8})$$

Equations (B-7) and (B-8) are identical to equations (54) and (55), respectively. Since by convention, anode potentials are greater than cathode,  $E_A$  will decrease exponentially and  $E_C$  will increase exponentially towards a final common potential  $E_f$  given by:

$$E_f = \frac{k_A E_{OC} + k_C E_{OA}}{k_A + k_C} \quad (\text{B-9})$$

Equation (B-9) is identical to equation (57). It is easily found from equations (B-7) and (B-8) by letting  $t \rightarrow \infty$ .  $E_f$  represents the steady state polarization potential.

The driving force  $\delta = E_A - E_C$  is found by subtracting equation (B-7) from equation (B-8), when:

$$\delta = (E_{OA} - E_{OC}) e^{-(k_A + k_C) t} \quad (\text{B-10})$$

Equation (B-10) is identical to equation (56). The driving force  $\delta$  decreases exponentially with time towards zero. Polarization is complete after a suitably long time and the final potentials of the anode and cathode are equal to the value predicted by equation (B-9).

## B.2 Equivalent Circuit Models

The models derived in this section treat the polarization process in terms of an equivalent electrical circuit [14]. Figure 3 is a schematic representation of the circuit. The anode and cathode are considered as being at opposite sides of a charged capacitor which has initial thermodynamic potential  $\delta_o = E_{OA} - E_{OC}$ . In the presence of an electrolyte this potential is dissipated across two resistances in series,  $R_1$  and  $R_2$ . Resistance  $R_1$  corresponds to the resistance of the electrolyte, which is assumed to be constant. Resistance  $R_2$  corresponds to the resistance offered by the corrosion products. In the first submodel (constant resistance)  $R_2$  is taken constant. In the other two models (Langmuir adsorption and uniform product accumulation) the resistance  $R_2$  increases with time.

Consider the circuit depicted in Figure 3. At time zero switch  $S_2$  is closed, switch  $S_1$  is opened and the circuit is complete. Application of Kirchoff's second law gives:

$$i (R_1 + R_2) + \frac{1}{C} \int_0^t i dt = 0 \quad (60)$$

or, since  $i = dQ/dt$ ,

$$(R_1 + R_2) \frac{dQ}{dt} + \frac{Q}{C} = 0 \quad (62)$$

The initial charge of the capacitor  $Q_o$  is given by:

$$Q = C \delta_o \quad (63)$$

Equations (60), (62) and (63) summarize the mathematical bases for the equivalent circuit models developed for polarization.

### B.2.1 Constant Product Resistance

When the products of corrosion have a constant product resistance  $R_2$ , equation (62) can be directly integrated to give:

$$\frac{Q}{Q_0} = \exp \left[ \frac{-t}{(R_1 + R_2) C} \right] = \exp \left[ \frac{-t}{\tau} \right] \quad (\text{B-11})$$

The product  $(R_1 + R_2) C$  is the polarization time constant  $\tau$ . Equation (B-11) predicts that the charge on the capacitor  $Q$  will decay exponentially with time towards zero with time constant  $\tau$ .

Since by definition  $i = dQ/dt$ , differentiation of equation (B-11) yields:

$$\frac{i}{i_0} = \exp \left( \frac{-t}{\tau} \right) \quad (\text{B-12})$$

where the initial current flow  $i_0$  is given by:

$$i_0 = \frac{\delta_0}{(R_1 + R_2)} \quad (65)$$

Applying Ohm's law:

$$\frac{i}{i_0} = \frac{\delta}{\delta_0} \quad (\text{B-13})$$

so that

$$\frac{Q}{Q_0} = \frac{i}{i_0} = \frac{\delta}{\delta_0} = \exp\left(\frac{-t}{\tau}\right) \quad (\text{B-14})$$

Equation (B-14) is identical to equation (64).

### B.2.2 Langmuir Adsorption of Corrosion Products

The development of this submodel is based upon the formation of an adsorbed film of reaction products at or in the vicinity of the electrode surface. The products can accumulate as a monolayer of adsorbed ions or in a diffuse double layer around the electrode. As the products build-up, their resistance  $R_2$  increases towards an ultimate value  $R_{2u}$ , corresponding to complete monolayer coverage.

The theory developed here is based on the classical Langmuir adsorption theory for the physical adsorption of gases [15]. Consider the electrode surface to contain a total number  $N_t$  of adsorption sites, and let  $N$  be the number of these sites which are occupied at any time  $t$ . Ions will adsorb onto the surface at a rate which is proportional to the number of unoccupied sites ( $N_t - N$ ) and desorb at a rate proportional to the number of occupied sites  $N$ . Writing the conservation law for ions arriving, leaving and being stored in the film:

$$\frac{dN}{dt} = k_a (N_t - N) - k_d N \quad (\text{B-15})$$

where

$k_a$  is the adsorption rate constant

$k_d$  is the desorption rate constant

Both rate constants have units of reciprocal time.

Let  $\frac{N}{N_t} = \theta$  be the fraction of the sites which are occupied. Then equation (B-15) can be rewritten as:

$$\frac{d\theta}{dt} = k_a (1 - \theta) - k_d \theta \quad (\text{B-16})$$

The equilibrium surface coverage  $\theta_e$  can be found by setting  $d\theta/dt = 0$  in equation (B-16):

$$\theta_e = \frac{k_a}{k_a + k_d} \quad (\text{B-17})$$

where  $0 < \theta < \theta_e < 1$

Substituting equation (B-17) into (B-16) and integrating using the fact that the surface is initially free of adsorbed ions:

$$\frac{\theta}{\theta_e} = 1 - \exp \left[ \frac{-k_a t}{\theta_e} \right] = 1 - \exp [ -(k_a + k_d) t ] \quad (\text{B-18})$$

Equation (B-18) predicts that the surface coverage will increase towards its final or equilibrium value  $\theta_e$ . If the adsorption process is irreversible then  $k_d = 0$ ,  $\theta_e = 1$  and equation (B-18) reduces to:

$$\theta = 1 - \exp (-k_a t) \quad (\text{B-19})$$

The resistance attributable to the film will be in direct proportion to the number of adsorbed ions. Thus:

$$\frac{\theta}{\theta_e} = \frac{R}{R_u} = 1 - \exp(-\alpha t) \quad (\text{B-20})$$

Equation (B-20) is identical to equation (58) of the text.

We can now identify precisely the meanings of the constants  $R_u$  and  $\alpha$  in equation (58) by analogy to the Langmuir adsorption theory. Thus, the ultimate resistance  $R_u$  corresponds to the equilibrium coverage  $\theta_e$  where the constant  $\alpha$  corresponds to the adsorption constant divided by the equilibrium coverage, i.e.,  $k_a/\theta_e$ .

Substituting equation (B-20) for  $R_2$  into Equation (62) a variables separable differential equation results, which on integration becomes:

$$\frac{Q}{Q_o} = \frac{\delta}{\delta_o} = \left[ \left( 1 + \frac{R_u}{R_1} \right) e^{-\alpha t} - \frac{R_u}{R_1} \right] e^{-\frac{t}{\alpha \tau_u}} \quad (\text{B-21})$$

$\tau_u$  is the modified time constant  $C(R_1 + R_u)$ . Equation (B-21) is identical to equation (67). The first equality in equation (B-21) results from the ratio of  $Q = C\delta$  and  $Q_o = C\delta_o$ . The capacitance of the electrochemical cell,  $C$ , is presumed constant.

Differentiating equation (B-21) and using the fact that  $i = dQ/dt$ :

$$\frac{i}{i_o} = \frac{\left[ \left( 1 + \frac{R_u}{R_1} \right) e^{-\alpha t} - \frac{R_u}{R_1} \right] e^{-\frac{t}{\alpha \tau_u}}}{1 + \frac{R_u}{R_1} (1 - e^{-\alpha t})} \quad (\text{B-22})$$

Equation (B-22) is identical to equation (68).

Dividing equation (B-21) by equation (B-22) and using (B-20):

$$\frac{\delta}{\delta_o} = \frac{i}{i_o} \left(1 + \frac{R_2}{R_1}\right) \quad (\text{B-23})$$

Equation (B-23) is identical to equation (70).

Large values of the constant  $\alpha$  correspond physically to rapid adsorption and/or desorption of adsorbed ions at the electrode surface (i.e. large  $k_a + k_d$ ), or to low equilibrium coverage (small  $\theta_e$ ) at high adsorption rates (large  $k_a$ ). Under these conditions equations (B-21) and (B-22) become equations (B-24) and (B-25), respectively.

$$\frac{Q}{Q_o} = \frac{\delta}{\delta_o} = \left(1 + \frac{R_u}{R_1}\right)^{-\frac{t}{\tau_u}} \quad (\text{B-24})$$

$$\frac{i}{i_o} = \left(1 + \frac{R_u}{R_1}\right)^{-(1 + \frac{t}{\tau_u})} \quad (\text{B-25})$$

Equations (B-24) and (B-25) are identical to equations (71) and (72). Equation (B-25) follows directly from Equation (B-24) and  $i = dQ/dt$ . Equation (B-24) can be found by the application of L'Hospital's rule to equation (B-21) as  $\alpha \rightarrow \infty$ .

### B.2.3 Accumulation of Solid Corrosion Products

If solid products of corrosion deposit or precipitate near or on the electrode surface then the resistance  $R_2$  caused by the accumulation of these products will increase with time. In some instances adsorbed films more than several monolayers thick can behave in a similar manner to solid corrosion products.

The resistance of the corrosion layer, if it remains homogeneous, will be proportional to this thickness. The volume of corrosion products laid down will be proportional to this thickness and by Faraday's law to the total amount of current which has flowed through the electrical circuit to any time  $t$ . Thus:

$$R_2 = \gamma \int_0^t i \, dt = -\gamma \int_0^t \frac{dQ_2}{dt} \, dt = \gamma (Q - Q_0) \quad (\text{B-26})$$

where

$\gamma$  is a rate constant for the accumulation of solid reaction products.

If equation (B-26) is substituted into equation (62), and the resulting variable separable differential equation is integrated, then it follows that:

$$\frac{Q}{Q_0} = \frac{\delta}{\delta_0} = \exp \frac{C\gamma (Q_0 - Q) - t}{C (R_1 + \gamma Q_0)} \quad (\text{B-27})$$

Equation (B-27) is identical to equation (73). It is a transcendental equation in the variable  $Q$  and thus must be solved by trial and error procedures in order to determine  $Q(t)$  and  $\delta(t)$ . The corresponding formula for the current ratio  $i/i_0$  is given by:

$$\frac{i}{i_0} = \frac{Q}{C [R_1 + \gamma Q_0 - \gamma \frac{Q}{Q_0}]} \quad (\text{B-28})$$

Equation (B-28) is equation (74).

Once  $Q(t)$  is known,  $R_2(t)$  can be found from equations (B-26) and (B-27).  $R_2(t)$  will in turn determine the relative thickness of the corrosion products attached to the electrode.

U.S. DEPT. OF COMM. <b>BIBLIOGRAPHIC DATA SHEET</b> <i>(See instructions)</i>	<b>1. PUBLICATION OR REPORT NO.</b> NBS TN 1150	<b>2. Performing Organ. Report No.</b>	<b>3. Publication Date</b> Sept. 1982
<b>4. TITLE AND SUBTITLE</b>  Mathematical Models for the Corrosion Protective Performance of Organic Coatings			
<b>5. AUTHOR(S)</b> James M. Pommersheim, Paul G. Campbell, and Mary E. McKnight			
<b>6. PERFORMING ORGANIZATION</b> <i>(If joint or other than NBS, see instructions)</i>  NATIONAL BUREAU OF STANDARDS DEPARTMENT OF COMMERCE WASHINGTON, D.C. 20234		<b>7. Contract/Grant No.</b>  <b>8. Type of Report &amp; Period Covered</b>  Final	
<b>9. SPONSORING ORGANIZATION NAME AND COMPLETE ADDRESS</b> <i>(Street, City, State, ZIP)</i>  Same as 6.			
<b>10. SUPPLEMENTARY NOTES</b>  <input type="checkbox"/> Document describes a computer program; SF-185, FIPS Software Summary, is attached.			
<b>11. ABSTRACT</b> <i>(A 200-word or less factual summary of most significant information. If document includes a significant bibliography or literature survey, mention it here)</i>  <p style="text-align: center;">           Mathematical models were developed for conceptual models describing the principal phenomena that occur in the corrosion performance of polymeric coatings. These include models for water and oxygen permeability through organic coatings, models for the growth of blisters beneath coatings, and preliminary models for the polarization occurring at the electrode surfaces. Results predicted by the models are discussed in terms of the improvement of the protective function of the membrane.         </p>			
<b>12. KEY WORDS</b> <i>(Six to twelve entries; alphabetical order; capitalize only proper names; and separate key words by semicolons)</i> absorption; adhesion; adsorption; conceptual models; corrosion; mathematical models; organic coating; osmosis; osmotic pressure; oxygen; permeability; pigment; protective performance; substrate; vehicle; water.			
<b>13. AVAILABILITY</b> <input checked="" type="checkbox"/> Unlimited <input type="checkbox"/> For Official Distribution. Do Not Release to NTIS <input checked="" type="checkbox"/> Order From Superintendent of Documents, U.S. Government Printing Office, Washington, D.C. 20402. <input type="checkbox"/> Order From National Technical Information Service (NTIS), Springfield, VA. 22161		<b>14. NO. OF PRINTED PAGES</b>  99 <hr/> <b>15. Price</b>  \$5.50	









# NBS TECHNICAL PUBLICATIONS

## PERIODICALS

**JOURNAL OF RESEARCH**—The Journal of Research of the National Bureau of Standards reports NBS research and development in those disciplines of the physical and engineering sciences in which the Bureau is active. These include physics, chemistry, engineering, mathematics, and computer sciences. Papers cover a broad range of subjects, with major emphasis on measurement methodology and the basic technology underlying standardization. Also included from time to time are survey articles on topics closely related to the Bureau's technical and scientific programs. As a special service to subscribers each issue contains complete citations to all recent Bureau publications in both NBS and non-NBS media. Issued six times a year. Annual subscription: domestic \$18; foreign \$22.50. Single copy, \$4.25 domestic; \$5.35 foreign.

## NONPERIODICALS

**Monographs**—Major contributions to the technical literature on various subjects related to the Bureau's scientific and technical activities.

**Handbooks**—Recommended codes of engineering and industrial practice (including safety codes) developed in cooperation with interested industries, professional organizations, and regulatory bodies.

**Special Publications**—Include proceedings of conferences sponsored by NBS, NBS annual reports, and other special publications appropriate to this grouping such as wall charts, pocket cards, and bibliographies.

**Applied Mathematics Series**—Mathematical tables, manuals, and studies of special interest to physicists, engineers, chemists, biologists, mathematicians, computer programmers, and others engaged in scientific and technical work.

**National Standard Reference Data Series**—Provides quantitative data on the physical and chemical properties of materials, compiled from the world's literature and critically evaluated. Developed under a worldwide program coordinated by NBS under the authority of the National Standard Data Act (Public Law 90-396).

NOTE: The principal publication outlet for the foregoing data is the Journal of Physical and Chemical Reference Data (JPCRD) published quarterly for NBS by the American Chemical Society (ACS) and the American Institute of Physics (AIP). Subscriptions, reprints, and supplements available from ACS, 1155 Sixteenth St., NW, Washington, DC 20056.

**Building Science Series**—Disseminates technical information developed at the Bureau on building materials, components, systems, and whole structures. The series presents research results, test methods, and performance criteria related to the structural and environmental functions and the durability and safety characteristics of building elements and systems.

**Technical Notes**—Studies or reports which are complete in themselves but restrictive in their treatment of a subject. Analogous to monographs but not so comprehensive in scope or definitive in treatment of the subject area. Often serve as a vehicle for final reports of work performed at NBS under the sponsorship of other government agencies.

**Voluntary Product Standards**—Developed under procedures published by the Department of Commerce in Part 10, Title 15, of the Code of Federal Regulations. The standards establish nationally recognized requirements for products, and provide all concerned interests with a basis for common understanding of the characteristics of the products. NBS administers this program as a supplement to the activities of the private sector standardizing organizations.

**Consumer Information Series**—Practical information, based on NBS research and experience, covering areas of interest to the consumer. Easily understandable language and illustrations provide useful background knowledge for shopping in today's technological marketplace.

*Order the above NBS publications from: Superintendent of Documents, Government Printing Office, Washington, DC 20402.*

*Order the following NBS publications—FIPS and NBSIR's—from the National Technical Information Services, Springfield, VA 22161.*

**Federal Information Processing Standards Publications (FIPS PUB)**—Publications in this series collectively constitute the Federal Information Processing Standards Register. The Register serves as the official source of information in the Federal Government regarding standards issued by NBS pursuant to the Federal Property and Administrative Services Act of 1949 as amended, Public Law 89-306 (79 Stat. 1127), and as implemented by Executive Order 11717 (38 FR 12315, dated May 11, 1973) and Part 6 of Title 15 CFR (Code of Federal Regulations).

**NBS Interagency Reports (NBSIR)**—A special series of interim or final reports on work performed by NBS for outside sponsors (both government and non-government). In general, initial distribution is handled by the sponsor; public distribution is by the National Technical Information Services, Springfield, VA 22161, in paper copy or microfiche form.

**U.S. Department of Commerce**  
National Bureau of Standards

Washington, D.C. 20234  
Official Business  
Penalty for Private Use \$300



POSTAGE AND FEES PAID  
U.S. DEPARTMENT OF COMMERCE  
COM-215

THIRD CLASS  
BULK RATE